Journal Of Solar Energy Science And Research

Volume No. 09

Issue No. 01

January - April 2025

ENRICHED PUBLICATIONS PVT.LTD

JE - 18,Gupta Colony, Khirki Extn,
Malviya Nagar, New Delhi - 110017.
E- Mail: info@enrichedpublication.com
Phone :- +91-8877340707

Journal Of Solar Energy Science And Research

Aims and Scope

The Journal of Solar Energy Science and Research is published quarterly by Enriched publications. Journal of Solar Energy Science and Research is peer reviewed journal and monitored by a team of reputed reviewers. Today, the journal continues to publish articles on topics ranging from solar radiation and solar materials to direct conversion of solar energy into electrical energy. In addition, readers will find important articles exploring other renewable energy sources. This journal places a strong emphasis on applications such as solar devices for home and industrial uses, solar heating and cooling systems, solar power systems and units, and agricultural uses of solar energy.

Journal Of Solar Energy Science And Research

Managing Editor
Mr. Amit Prasad

Journal Of Solar Energy Science And Research

(Volume No. 9, Issue No. 1, January - April 2025)

Contents

Computer Simulation Of Thin Layer Drying Of Tomato (Lycopersicon Esculentum L.) Slices

Amel A. Elmamoun* Hassan M. Adam* Haitham R. Elramlawi**

*Dept. of Agric. Eng., Faculty of Agriculture, University of Khartoum, Sudan.

** Center of Dryland Farming Research and Studies, University of Gadarif, Sudan.

ABSTRACT

Solar drying experiments in thin-layer of tomato slices were conducted at Shambat, Faculty of Agriculture, University of Khartoum, Sudan. The objectives were to test the performance of an indirect forced convective solar dryer, to determine the drying characteristics of tomato slices in winter season and to build a computer mathematical model based on Lewis and Page drying models to simulate thin-layer solar drying of tomato slices. Temperature and relative humidity measurements of ambient air, the inlet, outlet of solar collector and weight of tomato slices were recorded at intervals of one hour. Results indicated that the air inside the solar was heated adequately. The thin-layer solar drying of tomato slices showed that the drying characteristics of tomato slices such as moisture content, moisture ratio and drying rate decreased with increase of the drying time; the drying process took place during the falling rate period. The simulation model predicted the moisture contents of the thin-layer solar drying of tomato slices adequately, but Page model gave closer agreement between measured and predicted data. Statistical validation for the models showed that the coefficient of determination (R2) was 0.99 and 0.97 for Page and Lewis models, respectively. Root mean square error (RMSE) and Model efficiency (ME) were 0.00004 and 99% respectively for Page model and 0.031 and 97% respectively for Lewis model.

Key words: Lycopersicon esculentum L., Thin layer drying, Mathematical model.

1. Introduction

The postharvest loss in vegetables has been estimated to be about 30-40% due to inadequate postharvest handling, lack of infrastructure, processing, marketing and storage facilities (Karim and Hawlader, 2005). Drying of agricultural products may be one of the most important unit operations for the preservation of food materials (Rajput, 2005 and Sacilik et al., 2006). Diminishing reserves of fossil fuels and increased costs have led to a search for alternative energy sources including solar energy for drying agricultural products (Basunia and Abe, 2001; Pangavhane et al., 2002; Sacilik et al. 2006; Steinfeld and Segal, 1986 and Yadliz et al. 2001). Open-sun drying used to be an appropriate means in many urban and rural areas, but this conventional method cannot protect food materials from rain, dust, the attack by insects, birds and other animals. Therefore, it may increase the loss of products and have some

economic impacts on them (Pangavhane et al., 2002). Solar drying is a well-known food preservation procedure used to reduce the moisture content of agricultural products, which reduces quality degradation over an extended storage period (Midilli et al., 2002).

Tomato (Lycopersicon esculentum L.) is one of the most important fruits/vegetables grown in a wide range of climates, mostly in open-field but also under protection in plastic green houses and heated glass houses. It is a commercially important crop both for fresh fruit market and for the food processing industries. The annual worldwide production of tomatoes has been estimated at 125 million tons in an area of about 4.2 million hectares. The global production of tomatoes (fresh and processed) has been increased by 300% in the last four decades (FAO, 2005) and the leading tomato producers are in both tropical and temperate regions.

The thin layer drying procedure has been found to be the most appropriate tool for characterizing the drying parameters (Akgun and Doymaz 2005; Akpinar et al., 2003a and Akpinar et al., 2003b). Currently, there are three types of thin layer drying models to describe the drying rate of agricultural products, namely, theoretical, semi- theoretical and empirical models (Demirats et al., 1998 and Midilli et al., 2002). The theoretical approach concerns either the diffusion equation or simultaneous heat and mass transfer equations. The empirical model neglects the fundamentals of dryingprocesses and presents a direct relationship between average moisture and drying time by means of regression analysis (Ozdemir and Devres 1999). Also, the semi-theoretical model is a trade-off between the theoretical and empirical ones, derived from a widely used simplification of Fick's second law of diffusion or modification of the simplified model, such as the Lewis model, the Page model and the Modified Page model (Table 1).

Table 1. Lewis, Page and Modified Page models

Model name	Model equation
Lewis	$MR = \exp(-kt)$
Page	$MR = \exp(-kt^n)$
Modified Page	$MR = \exp(-kt)^n$

where:

MR = is the moisture ratio (dimensionless)

t = is the dried time (min.)

k and n = constants.

Materials And Methods

Solar drying experiments were carried out at Shambat, Department of Agricultural Engineering, Faculty of Agriculture, University of Khartoum, during December 2013 – January 2014. Thin- layer drying experiments were conducted to generate constants required for model validation in winter season under Shambat conditions (Sudan). The tomato slices (5 cm thickness) were placed in the drying chamber of the solar dryer and periodically weighed using a sensitive balance at hourly intervals from 8:30 am till 17:30 pm to determine the weight loss.

Also, dry bulb temperatures (oC) and Relative humidity (%) at the inlet, outlet of solar collector, ambient air and drying chamber were measured and recorded by the thermohygrometer. Drying process was continued for three days until the sample reached constant weight.

Construction of solar collector

The forced convective solar dryer used in this study was previously constructed for a research work. The solar dryer consists of a solar collector and a drying chamber. The solar collector consists of two boxes. The first box was 100 cm x 100 x cm 20 cm and it was made of wooden sides. It consists of a metal-plate base painted in non-shine black paint so as to absorb maximum solar radiation. A glass sheet (100 cm x 100 cm x 0.3 cm) was used to cover the box in order to minimize the loss of heat energy collected and to improve the solar dryer efficiency. The glass sheet was fixed tightly to the top of the solar collector by a silicon rubber, which allows the glass sheet to expand and contract due to the temperature fluctuations. The first box was placed inside a second box made of a metal frame and the sides were covered with wooden board. The second box had the same shape of the first box, but larger in dimension (114 cm x 114 cm); the gap between the two boxes was filled with fiber glass as insulation layer, so as to minimize the heat losses to the surrounding. All outsides of the outer box were painted in black in order to prevent the reflection of solar radiation. The drying chamber was attached to the upper opening of the solar collector by tube. It consisted of two cylinders. The out cylinder was 22 cm in diameter and 35 cm in height and it was welded at the bottom to that tube comes from the solar collector out let. The inner cylinder was 25 cm in diameter and 25 cm in height; it was movable and it had a detachable perforated base for the ease of taking the measurement. The two cylinders were designed to have a gap between their bases so as to guarantee uniform distribution of the hot air through the material to be dried .The solar collector was oriented to south and tilted to form an angle 15° with ground surface

Results And Discussion

Drying conditions of the solar dryer

Fig 1 showed temperatures of ambient air, inlet and outlet of solar collector and drying chamber of solar dryer for three successive days of the drying process of tomato slices. The four temperatures start to increase from the morning, reach the maximum at the noon and then decrease in the evening. From the Fig 1 it is clear that outlet of solar collector (heated air) and ambient air temperatures are close to each other at 8:30. The average difference between heated air and ambient air temperature is about 5.03oC at 8:30 a.m. The maximum average different is 28.1oC at noon (13:30) p.m. There is still average different temperature of 9.8oC between heated air and ambient air temperature at 17:30 p.m. This shows that, the drying air heated by the solar collector satisfactorily in order to increase its capacity for picking up moisture. This is inagreement with the result of Ayoub (2006) and Ibn Idris (2007). Fig 2 shows the ambient air, inlet and outlet of solar collector relative humidity over the three days of drying process of tomato slices. The relative humidity has a zigzag shape and fluctuates during the day hours of the drying process. All air relative humidity start to decrease from the morning reaching minimum at the noon then increase towards evening. The maximum attained relative humidity difference between average ambient and outlet of the solar collector air relative humidity is 10.2%. This also confirms that, the drying air is heated by the solar collector satisfactory in order to increase its capacity for taking up moisture. This is also in agreement with the result of Ayoub (2006) and Ibn Idris (2007).

Fig 3 shows temperature and relative humidity of the heated air. As shown in the figure as average temperature of heated air increases its average relative humidity decreases and vice versa. Generally, the two curves converge at morning diverge at noon and then converge again at evening. This could be due to fact that at noon, the solar collector had absorbed sufficient heat, which resulted in raising the temperature of the drying air. In addition, if the temperature of the air increases, while its absolute humidity (moisture content of air) is constant, its relative humidity will decrease. This finding agrees with that Ayoub (2006) in the drying of tomato.

Drying Characteristics Of Tomato Slices

Figures 4 and 5 show the drying curves of tomato slices and they were obtained by plotting moisture content versus drying time and moisture ratio versus drying time respectively. From these curves it is clear that the drying process take place in the falling rate period .This result is in agreement with finding of Ayoub (2006). Also, it is clear that at the end of the first day and continuing through the second and third days of the drying process an equilibrium state, regarding drying of tomato slices, was attained.

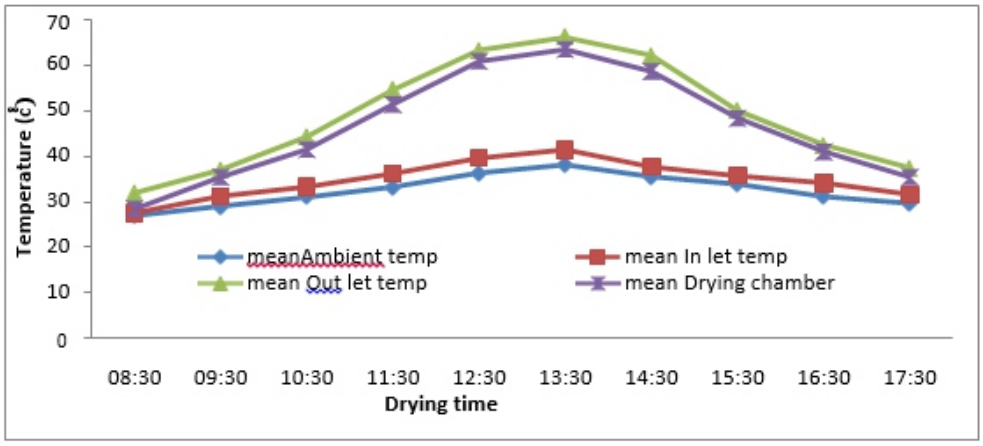

Fig 1. Mean inlet, outlet of solar collector, ambient and drying chamber temperatures

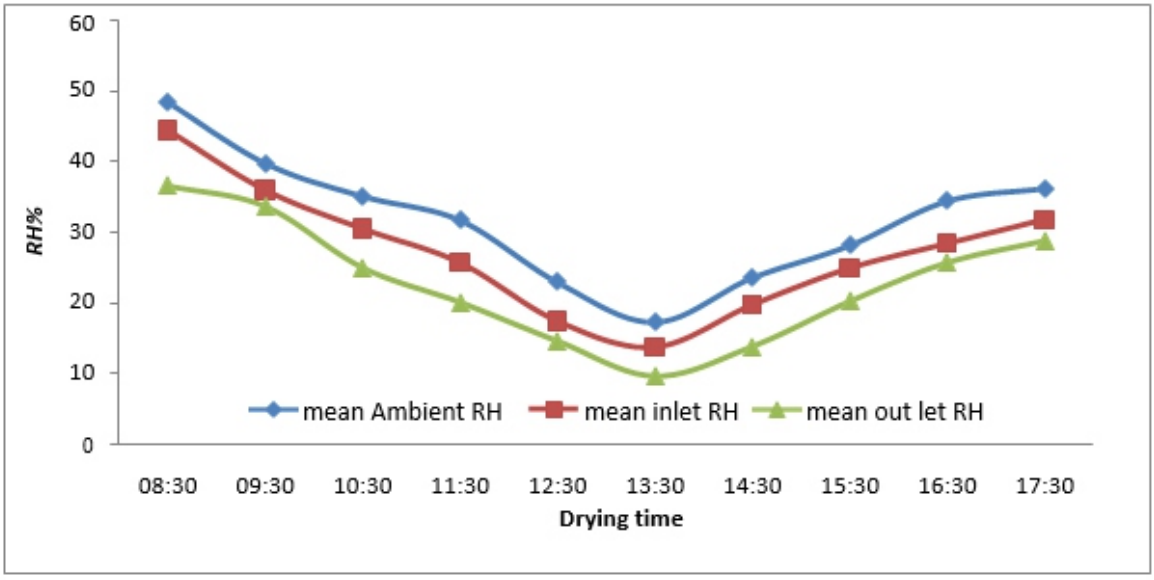

Fig 2. Mean inlet, outlet and ambient relative humidity of heated air

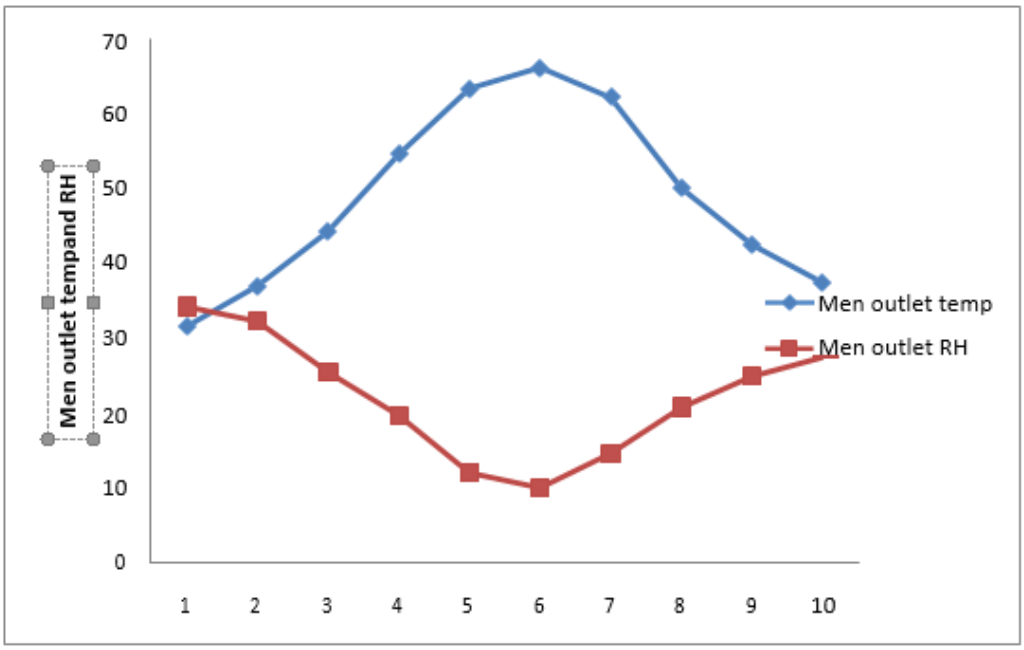

Fig 3. Heated air temperature and relative humidity versus drying time

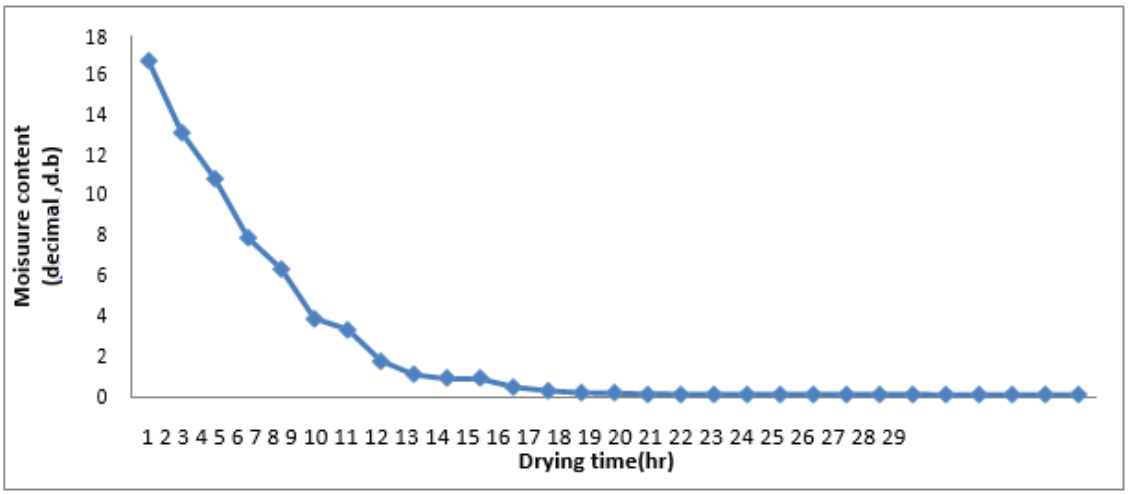

Fig 4. Variation of moisture content with drying time of tomato slices

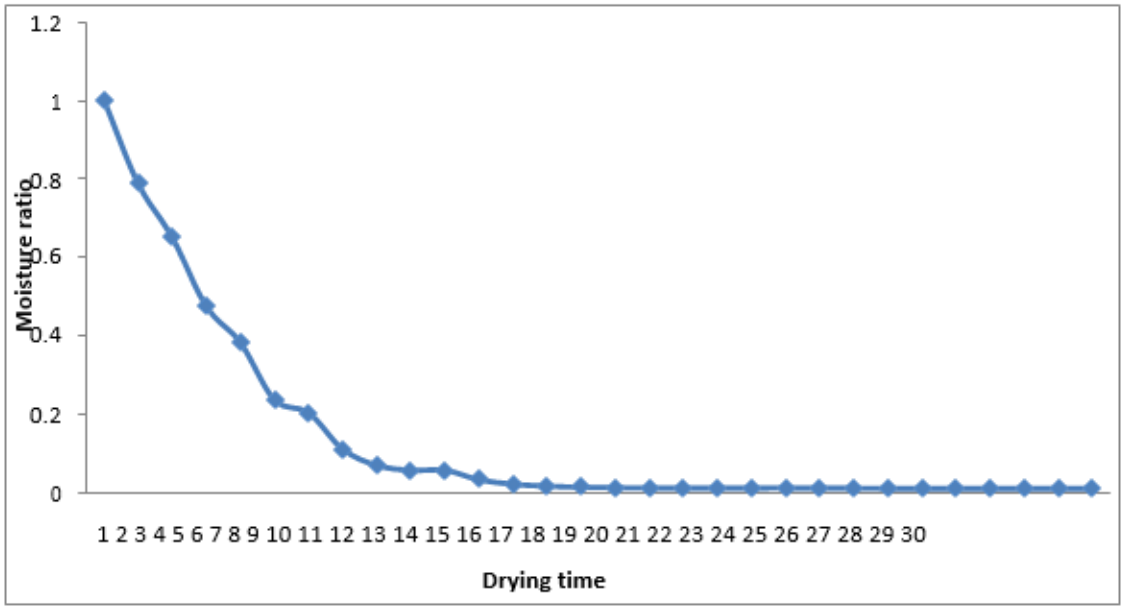

Fig 5. Variation of moisture ratio with drying time tomato

Validation of the two tested drying models

The drying constants for the two tested drying models namely; Page and Lewis models addition to the exponent (n) in Page model were obtained using data transformation and linear regression techniques as shown Figures 6 and 7, respectively. Table 2 shows the drying constant and coefficient of two tested drying models. Computer program output of the predicted tomato moisture contents and moisture ratio of a Thin-layer drying of tomato slices of Page and Lewis models are shown Table 4.

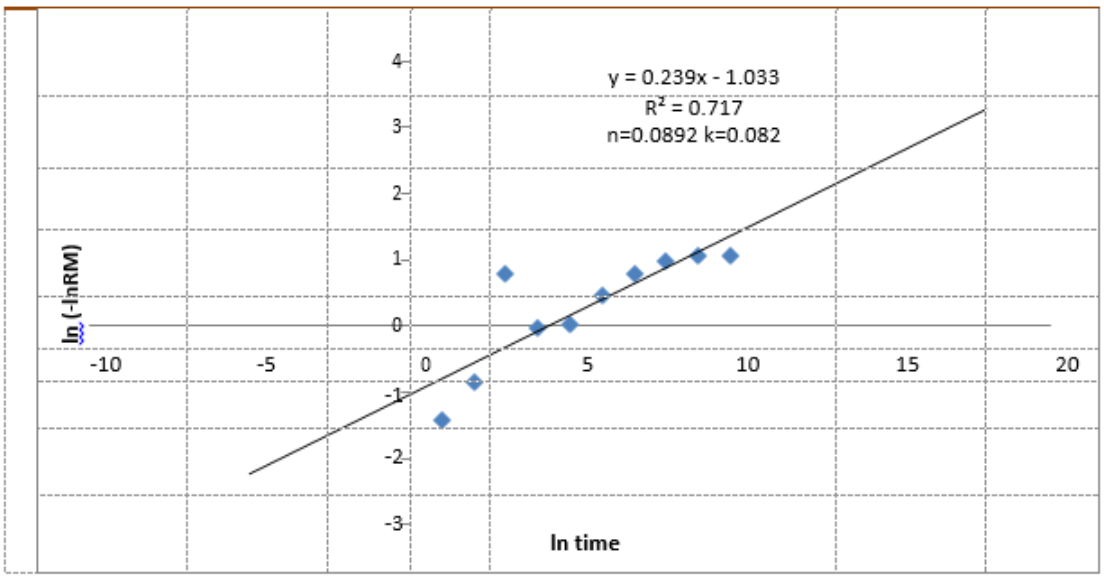

Fig 6. Calculation of the coefficient for Page model

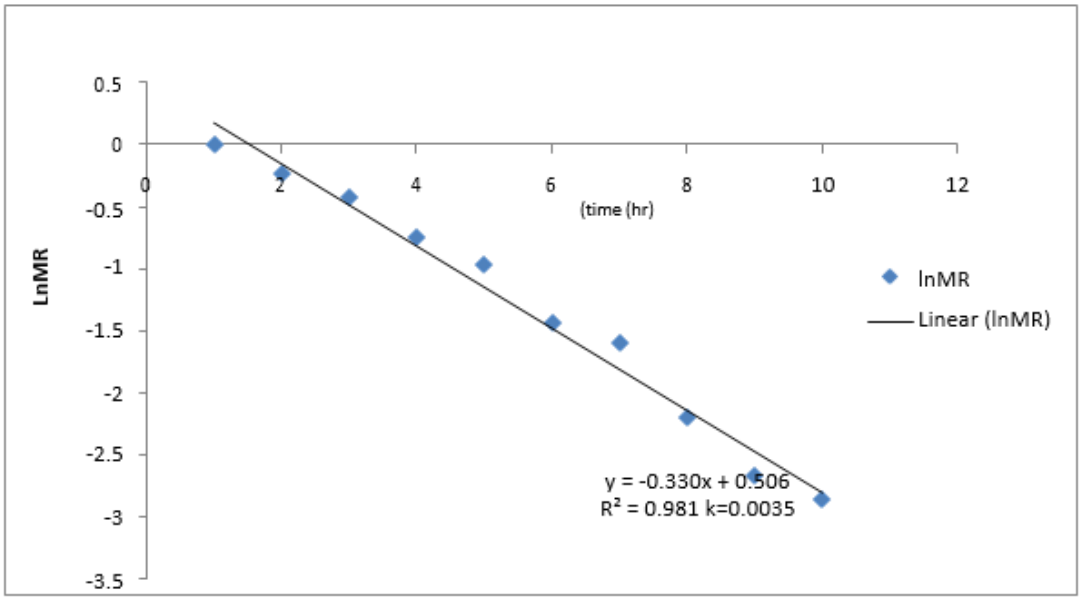

Fig 7. Calculation of the coefficient for Lewis model

Table 2. The drying constants and coefficients of the two tested drying models

Drying model name	Drying constants and coefficients
Lewis	K = 0.0035
Page	K = 0.0082
	n = 0.0892

Graphical Validation Of The Two Drying Models

Fig 8 shows the measured and predicted moisture contents of Thin-layer of tomato slices by the two drying models. Generally, the two models predicted tomato slices moisture ratio and moisture content satisfactorily but Page model gave a close agreement between measured and predicted data

Tomato Quality

Plate 1 shows the difference in color and general appearance between the sun dried and solar dried tomato slices. As shows the color of the tomato slices indicates its Lycopene content. General appearance of the solar dried tomato slices seems more bright and clean and slices preserved their natural color drying. Ayoub (2006) concluded that when tomato dried by direct sun drying the resulting product is often insect-infested and sand covered all this lead to clean dried.

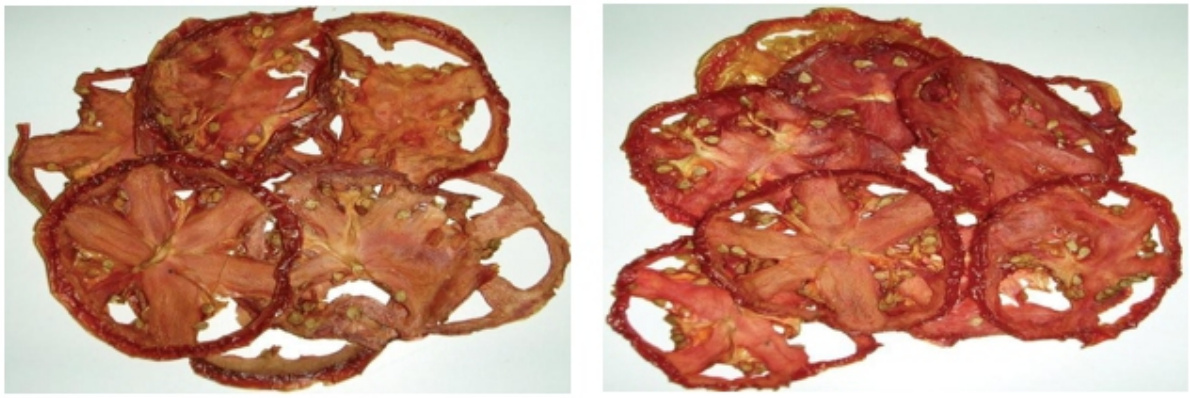

(a) (b)

Plate 1. Comparison between (a) open-air dried tomato slices (5mm) and (b) solar dried tomato slices (5mm)

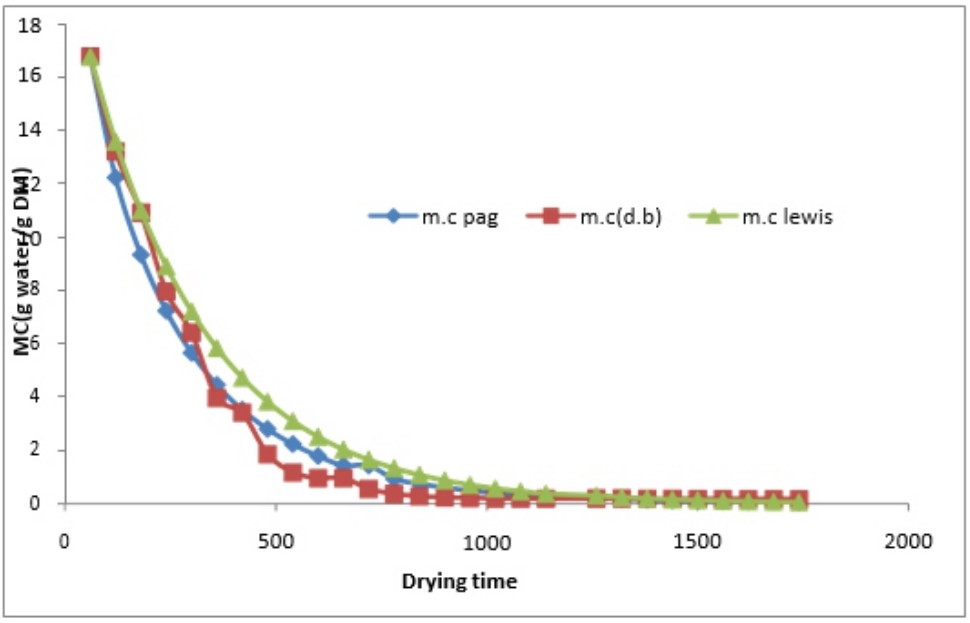

Fig 8. Measured and predicted moisture content of tomato

Statistical analysis

Figures 9 and 10 show the plotting of predicted moisture ratio versus experimental one of Lewis and Page models, respectively. Its clear that Page model gave the highest R^2 (0.99). Table 3 depicts the statistical validation parameters concerning both Page and Lewis drying models. With regard to Page

model; the root mean square errors (RMSE), determination coefficient (R^2) and model efficiency (ME) are 0.0004, 0.99 and 99%, respectively. While for Lewis model the parameter is 0.031, 0.97 and 95%, respectively. These values show that the two tested drying models predicted of tomato slices moisture ratio and moisture contents accurately but Page prediction is in close agreement with measured data. The ME and R^2 of the Page model was higher than that obtained from Lewis and tends to be one. The RMSE were lower for the Page model than that obtained from Lewis model tend to be zero.

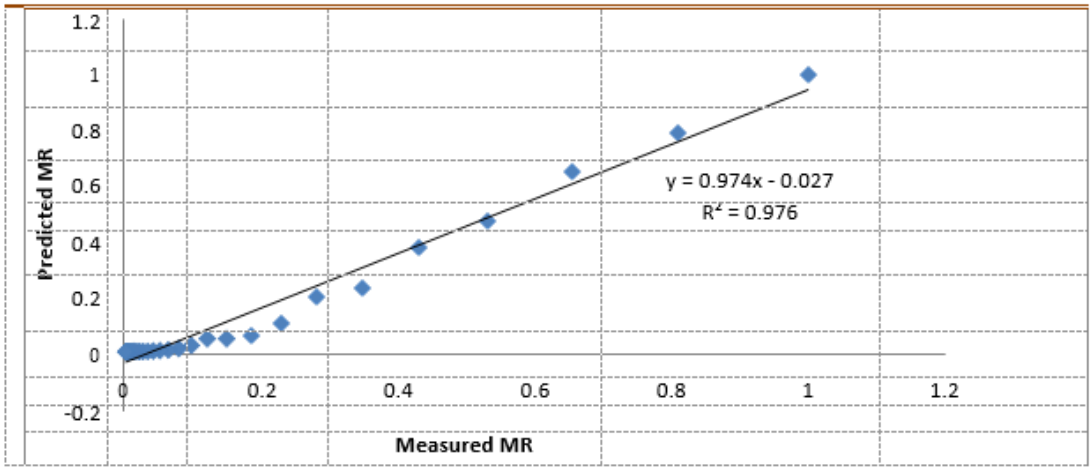

Fig 7 Lewis model predicted MR versus measured MR

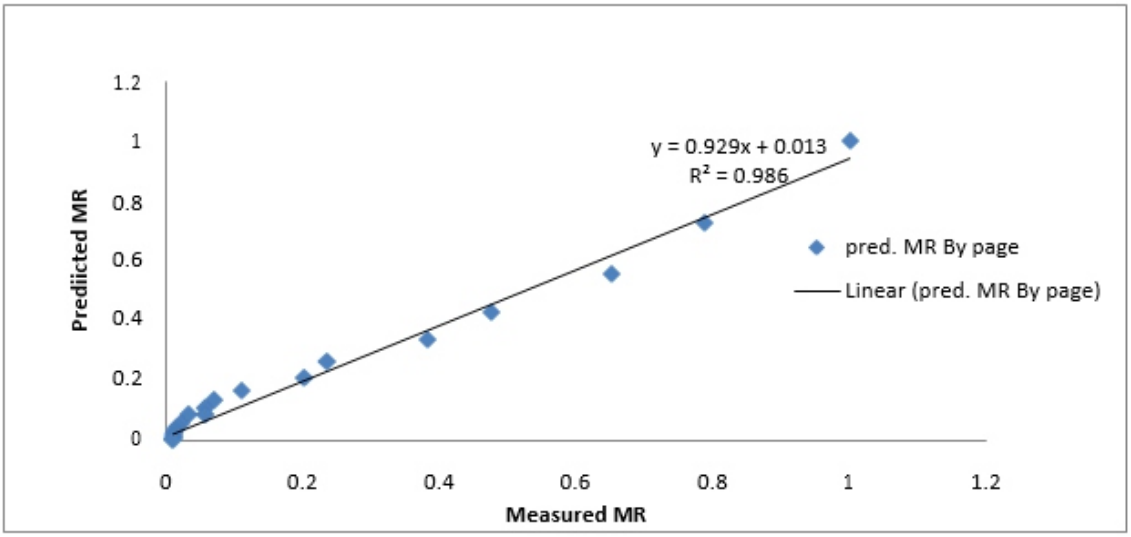

Fig 8 Page model predicted MR versus measured MR

Table 3. Determination coefficient, root mean square error and model efficiency of estimate between measured and predicted moisture ratio

Statistical parameters / Model name	Determination coefficient( )	Root mean square error and model	Model efficiency %
Page	0.99	0.0004	99
Lewis	0.97	0.03	95

Table 4. Computer output of the predicted tomato moisture contents and moisture ratio of a Thin-layer drying of tomato slices of Page and Lewis models

Time (min)	Measured MR	pred. MR By Lewis	pred. MR By Page	Measured m.c	Pred. m.c by Pages model	Pred. m.c by Lewis model
0	1	1	1	16.8	16.8	16.8
60	0.78811	0.809814525	0.729253353	13.2379	12.2515	13.60488
120	0.651004	0.655799564	0.556648618	10.9349	9.351697	11.01743
180	0.474835	0.531076012	0.431280354	7.97578	7.24551	8.922077
240	0.382817	0.430073068	0.337244379	6.43015	5.665706	7.225228
300	0.236515	0.348279417	0.265468747	3.97274	4.459875	5.851094
360	0.203774	0.282041731	0.210050512	3.42278	3.528849	4.738301
420	0.111039	0.22840149	0.166901862	1.86512	2.803951	3.837145
480	0.069923	0.184962844	0.133087277	1.1745	2.235866	3.107376
540	0.057138	0.149785598	0.10644788	0.95974	1.788324	2.516398
600	0.057167	0.121298553	0.085368904	0.96022	1.434198	2.037816
660	0.033076	0.09822933	0.085368904	0.55557	1.434198	1.650253
720	0.021981	0.079547538	0.055286884	0.36921	0.92882	1.336399
780	0.01671	0.064418752	0.044626437	0.28067	0.749724	1.082235
840	0.01414	0.052167241	0.036085652	0.23751	0.606239	0.87641
900	0.012846	0.042245789	0.029227262	0.21577	0.491018	0.709729
960	0.011764	0.034211254	0.023708305	0.19759	0.3983	0.574749
1020	0.01142	0.02770477	0.019258662	0.19182	0.323546	0.46544
1080	0.011248	0.022435725	0.015664809	0.18893	0.263169	0.37692
1140	0.01164	0.018168776	0.012757401	0.19551	0.214324	0.305235
1200	0.011712	0.014713339	0.010401742	0.19672	0.174749	0.247184
1260	0.011206	0.011915076	0.008490412	0.18822	0.142639	0.200173
1320	0.011073	0.009649001	0.006937531	0.186	0.116551	0.162103
1380	0.010685	0.007813901	0.005674295	0.17947	0.095328	0.131274
1440	0.010398	0.006327811	0.004645461	0.17466	0.078044	0.106307
1500	0.010198	0.005124353	0.003806597	0.1713	0.063951	0.086089
1560	0.010169	0.004149776	0.003121899	0.17081	0.052448	0.069716
1620	0.01016	0.003360549	0.002562469	0.17065	0.043049	0.056457
1680	0.01016	0.002721421	0.002562469	0.17065	0.043049	0.04572
1740	0.01016	0.002203846	0.002104949	0.17065	0.035363	0.037025

References

Akgun, N. and Doymaz, I. (2005). Modeling of Olive Cake Thin-layer Drying Process. J. Food Eng., 68: 455-461.

Akpinar, E. K.; Bicer, Y. and A. Midilli, (2003a). Modeling and Experimental Study on Drying of Apple Slices in a Convective Cyclone Dryer. J. Food Proc. Eng., 26(6): 515-541.

Akpinar, E.K.; Bicer, Y. and Yildiz, C. (2003b). Thin Layer Drying of Red Pepper. J. Food Eng., 59: 99-104.

Ayoub, A.A. (2006). Mathematical modeling of solar drying of tomato slices. Ph.D. Thesis University of Khartoum.

Banerjee, R. (2005). Capacity building for Renewable Energy in India. Proceedings of International congress on Renewable Energy (ICORE 2005), January, Pune India, pp. 77-83.

Basunia, M.A. and Abe, T. (2001). Thin Layer Solar Drying Characteristics of Rough Rice under Natural Convection. J. Food Proc Eng., 47(4): 295-301.

Davies, J.N. and Hobson, G.E. (1981).The constituents of tomato fruit - The influence of environment, nutrition, and genotype. CRC critical Reviews in Food Science and Nutrition, 15: 205-280.

Demirats, C., Ayhan, T. and Kaygusuz, K. 1998. Drying Behavior of Hazelnuts. J. Sci. Food Agri., 76: 559-564.
FAO, (2005). Homepage: http://www.fao.org.
Ibn Idris, E. M. (2007). Modeling of Thin-layer solar drying of okera pods. Unpublished M.Sc. Thesis University of Khartoum.
Karim, M.A. and Hawlader, M.N.A. (2005). Mathematical modelling and experimental investigation of tropical fruits drying. International Journal of Heat and Mass Transfer, 48: 4914-4925.
Midilli, A.; Kucuk, H. and Yapar, Z.A. (2002). New Model for Single-layer Drying. Dry. Technol., 20(7): 1503-1513.
Okos, M.R.; Narasimhan, G.; Singh, R.K. and Witnaurer, A.C. (1992). Food Dehydration. In .R. Hedman and D.B.L und (Eds.). Handbook of Food Engineering, New York, Marcel Dekker.
Ozdemir, M. and Devres, Y. (1999). The Thin Layer Drying Characteristics of Hazelnuts during Roasting. J. Food Eng., 42(4):225-233.
Pangavhane, D.R.; Sawhney, R. and Sarsavadia, L. (2002). Design, Development and Performance Testing of a New Natural Convection Solar Dryer. Energy, 27: 579- 590.
Rajput, R.K. (2005). A Textbook of Power Plant Engineering. Laxmi Publications, New York. Sacilik, K.; Keskin, R. and Elicin, A. (2006). Mathematical Modeling of Solar Tunnel Drying of Thin Layer Organic Tomato. J. Food Eng., 73: 231-238.
Steinfeld, A. and Segal, L. (1986). A Simulation Model for Solar Thin Layer Drying Process. Dry. Technol., 4: 536-554.
Yadliz, O.; Ertekin, C. and Uzun, H.I. (2001). Mathematical Modeling of Thin Layer Solar Drying of Sultana Grapes. Energy, 42: 167- 171.

Indirect Source Of Solar Energy Conversion- Sustainable Biomass And Biogas

Pawan Malik *

*Department Of Chemistry,S.L Bawa D.A.V. College, Batala (Gsp)Punjab,INDIA

ABSTRACT

In our industrialized society, it is quite difficult to maintain adequate supply of energy. As we all already know, fossil fuels are declining year by year, there is dire need to search alternative source of renewable energy. Various factors like rising population and shortage of commercial fuels in rural and traditional sectors have sustained the growing use of biomass as energy. One of most common alternative source of energy is Biomass. There are several source of converting biomass into biogas and many useful products. An attempt has been made to study on various sources such as water hyacinth, algae, grass, trees etc. The study emphasis on methods to generate biogas for cooking and lighting. Biomass plays an important role to act as renewable energy and assume to be best substitute for use of fossil fuels. Biomass proves to be solving many environmental issues especially global warming, reducing green house gas emission and sustainable development among poor nations. The study reveals the various types of biogas unit used in India such as floating and fixed dome type biogas plant and compares it with other biogas unit available in the market. No doubt, energy from biomass is more reliable as it is free from fluctuation like wind energy.

Keywords: Solar Energy; Biomass ; Sources; Biogas unit; Energy generation

1. Introduction

Solar energy is the ultimate source of most forms of energy and widely used as clean, safe and viable quantities in many parts of world. Sun's energy has been used by both nature and man to synthesis food. Its energy is utilized in power refrigerators and help to operate pumps, sewage treatment plants. Solar energy can be trapped as heat called photo thermal process or can be directly undergo electric conversion called photovoltaic process. Other process such as photochemical in which solar energy is stored in the form of chemical energy. In this mode, energy is utilized in atomic and molecular system which undergoes chemical changes and result in the formation of biomass. This biomass is further processed to produce more convenient gaseous or liquid fuels. The overall pathways for biomass generation can be described as-

Solar energy ⟶ Photosynthesis ⟶ Biomass ⟶ Energy generation

In this mechanism, the first step to produce biomass is the trapping of sunlight to produce sugar and starches from plants through the process of photosynthesis. For biomass generation, photosynthesis is the biological conversion of solar energy into carbohydrates and energy rich compounds. Intensity of solar light having wavelength around 400-700A0 is an important requirement for generating carbohydrates [1]

$$\text{Light} + CO_2 + H_2O \longrightarrow \text{Carbohydrate} + O_2 \text{ (Photosynthesis)}$$

The oxygen liberated is from H_2O and not from CO_2 molecule. This process is called CO_2 assimilation. CO_2 is an essential requirement for the growth of plant. In normal healthy atmosphere, the concentrations of CO_2 is 0.03-0.04%. The increase in concentration of CO_2 can be achieved by animal respiration, by using organic manure, by combustion of fossil fuel. Such a technique of harnessing solar energy into renewable form of energy which is used in domestic purposes.

The term "Biomass" includes all plant life- Trees, Bush, algae, agricultural crops and their residue. The residue means crop residue or agro processing residue such as husk, molasses, oilseed shells, sawdust etc. Biomass also includes human excreta, household waste, industrial waste or sewage sludge. The resources of biomass can be categorized as:

(i) Traditional solid mass i.e. wood and agricultural residue.

(ii) Non-Traditional form.Traditional solid mass can be burned directly to produce energy while Nontraditional form is converted to ethanol and methanol, used as liquid fuel in engines. When this biomass undergoes an aerobically fermented, it produces gaseous fuel called biogas. Earlier, biogas is produced from domestic and farmyard waste and gets utilized in rural areas. There are generally three ways to obtain energy from biomass. These may be thermo chemical route, biochemical route or oil extraction. In thermo chemical route, it includes process like combustion, gasification and pyrolysis. Combustion generally proceeds with complete burning of biomass to heat and power. In combustion, wood, agricultural waste, dung waste are most commonly used fuel. For better result, some special species of trees such as Eucalyptus, babool,casuarinas are grown and harvested at regular interval of time so that wood is available all the season for cooking purposes[2]. Gasification involves burning of solid biomass in limited supply of air while Pyrolysis is the process of burning of biomass at very high temperature in the absence of oxygen and result in the formation of charcoal and high volatile gaseous products.

Materials for Biomass production: There is long list of sources of biomass generation. The material generally used is cow dung and poultry droppings which are conveniently converted into biogas. Many other material such as algae, crop residue, agro waste, paper waste, human waste, trees or any cellulosic material of animal or plant origin are used for generation of biogas. There are some important sources of biomass summarized in the figure 1.

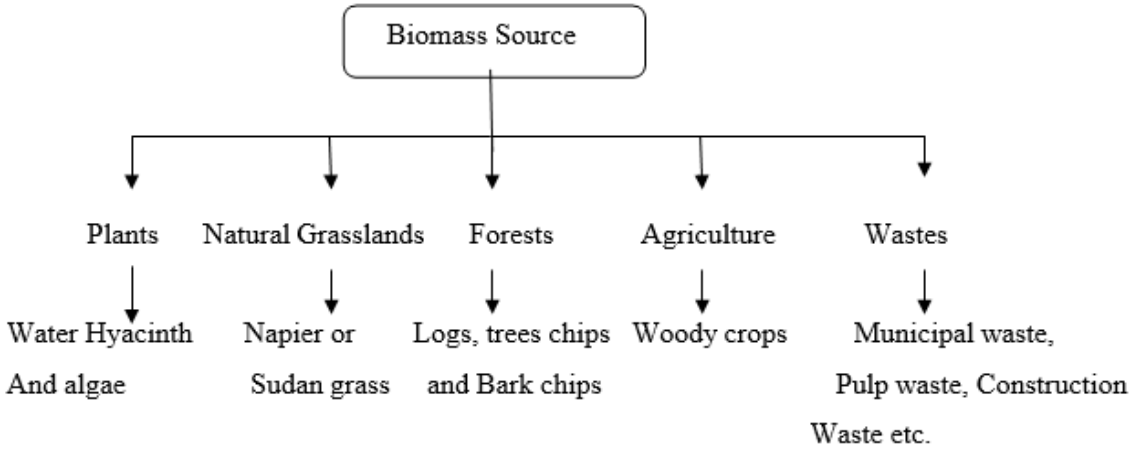

Fig.1 Biomass Source

1. **Water Hyacinth:** Water hyacinth is a major source of biomass which can be converted into methane and used as a nutritive food. It is generally found in rivers of hot region of world. This water plant is fresh water macrophyte and botanically named as: Eichhonia Crassipes" as in figure 2. The study reveals that anaerobic filter digester produce 130 litres of methane per one kilogram of volatile solids for 10 days and biogas produce contain approximately 65% methane [3]. Water hyacinthproduce 350 to 450 litres of biogas per kg of dung solids.

Fig. 2 Water Hyacinth

Water hyacinth is used as good food, fertilizers and biogas producer. It is also used in paper production. This floating plant can be used as feedstock for local energy production and produce important products with special environmental and ecofriendly sustainable benefits. Water hyacinth has rich in quantity of cellulose, lignin etc. which is much lesser in cow dung (locally practiced energy production process). Thus, this plant not only produce methane gas which is used for cooking but its residue after digestion provide fertilizer rich in nutrients [4]

2. Algae: Algae is single cell plant which has high protein content. Algae are generally grown on open setting ponds, but its yield is much poor. Some varieties such as ulothoria, spiruiina, scenedesmus have higher yield. Algae can be burned directly or an aerobically fermented to produce methane. Generally,

dry algae can produce 3300 Kcal per kg. Algae biofuels are nontoxic and biodegradable. They contain no sulphur and produce energy as much when we compare with conventional fossil fuels [5].

3. Natural Grasslands: Agronomically managed, perennial grasslands produce higher biomass yield. Perennial warm season tall grasses are potential source of better yield and quality. These grasslands assumed to be lower operating cost than Convention row crops and thereby reducing fuel and labour expenses[6] These grasses need much less water than marine plants and secondly, they are periodically harvested leaving the stubbles to grow again. Grass species such as Napiergrass, Sudan grass give best yield. Here is given natural grassland in figure 3 These grasses after cutting get dried and compacted to be used as fuel or mixed with water to form slurry to be introduced in biogas digesters.

Fig. 3 Natural Grassland

4. Trees: The most prominent source of wood is trees. By using solar energy, wood be burned in boilers for power production. Actually, wood is free from sulphur and ash obtained after burning can be used as fertilizers. Some species of tree with their biomass are given in Table 1 as:

Table 1: Trees with biomass yield

Species	Yield (tone/acre/year)
Eucalyptus	24.1
Sycamose	11.2
Conifers	5.4
Cotton wood	3.1

Out of the above, Eucalyptus has maximum yield rate. These trees are cut for wood and stumps grow back to size before next cutting.

5. Agriculture: Crops are grown specifically as a fuel and provide high output per hectare. The byproducts are agriculture residue, important energy conversion technology. This agriculture residue may be dry residue such as husks, animal manure or slurries, poultry litter. Wet residue includes animal slurry and farmyard manure or grass silage. Care must be taken when using wet residue, moisture content must be removed before digestion otherwise it reduces energetic efficiency. Also in gasification process, there must be minimum moisture content.

6. Waste: Waste includes Municipal solid waste such as oil/fats, pulp waste, construction material waste which are produced from industry or other domestic operation. These waste and residue has

valuable energy content [7]. Many industrial byproducts can be converted into biomass fuel. Industrialized waste can be woody or nonwoody waste. Woody waste could be wood composites, untreated wood. Nonwoody waste includes paper pulp, sewage sludge or textile, can be potentially used as biomass fuel.

Conversion of biomass into energy-Biogas plant: In India, biogas technology starts in the year 1937 when municipal sewage sludge undergoes anaerobic digested. There are various types of material used for biogas generation such as cow dung, waste include wet organic waste. When wet organic waste is undergone digested, it produces 50% methane. The composition of biogasdepends upon digestion process. In normal digestion process, biogas has methane concentration 55-75%. Typical composition [8] of biogas are summarized in table 2.

Table 2: Composition of biogas

Compound	Percentage
1. Methane(CH_4)	50-75
2. Carbon dioxide(CO_2)	25-50
3. Nitrogen(N_2)	0-10
4. Hydrogen(H_2)	0-1
5. Hydrogen sulphide (H_2S)	0-3
6. Oxygen(O_2)	0-0

There are various types of biogas unit developed which subsequently improved and designed at different stages. Earlier, Khadi and village industry (KVIC) developed a floating dome shaped biogas plant (called as Grah Luxmi).

1. Khadi and village industry (KVIC) Biogas type: In KVIC type, there is basically two basic components a) digester pit b) Dome. Digester is a well containing animal waste in the form of slurry and dome is that which floats on slurry and act as gas holder. The container at which digestion of sludge containing a large amount of complex organic matter (carbohydrates, proteins, fats) takes place at ambient temperature of 35-700 C is called digester and process is called anaerobic digestion. The flow chart of anaerobic digestion takes place as in figure 4.

After the complex organic molecule undergoes enzymatic hydrolysis, it breaks down into simple organic molecule, it passes through two stages:

I) Acid fermentation: Simple organic substances in waste are acted upon by special kind of bacteria

called acid former which broke up into simple acids.

ii) Methane Formation: These simple acids are again acted upon by bacteria to produce methane and carbon dioxide [9].

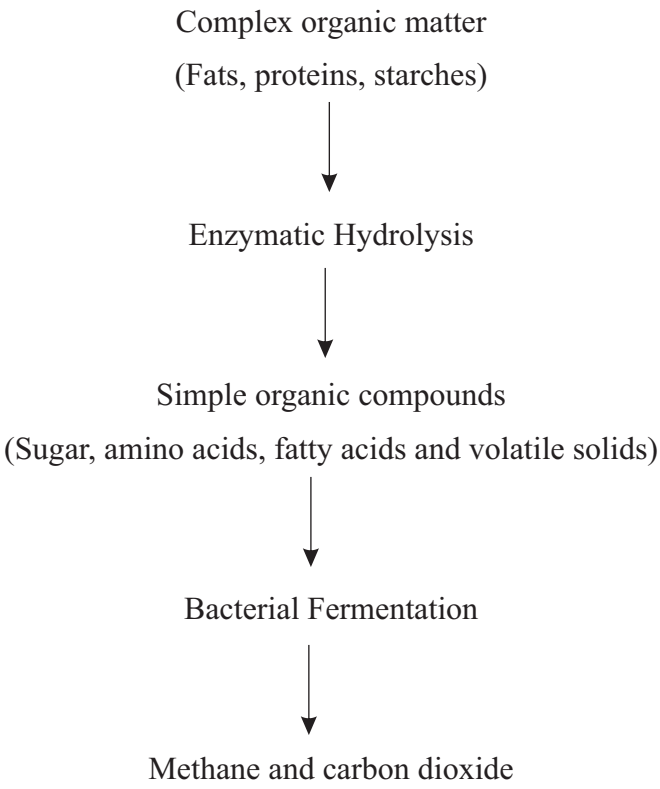

Fig.4 Anaerobic Digestion

The biogas generated has calorific value around 16000 to 25,000 kj/m3.It is excellent fuel for cooking and lighting. For efficient generation of biogas, Following are condition:

- There should be pH value around 6.5-8 for efficient production of biogas.
- Optimum temperature must be between 35-380 C for working of methane bacteria. Lowering the temperature, lesser will be the yield of biogas and even production will be stopped at a temperature of 100C.
- A specific ratio of carbon to nitrogen (C/N) must be kept between 25:1. Normally 1 Kg of dry cattle requires 1000 ml of eater to produce 1 m3 of biogas.

Working of KVIC: It consists of a digester which is made of masonry work and built below the ground level. There is partition wall in the centre which divide digested well vertically into two semi

cylindrical compartments. There are two slanting cement pipes for inlet and outlet purpose. A mixing of cow dung and water in the ratio of 4:5 flows through inlet pipe into digester as in figure 5. When both the compartments of digester pit are full, then equivalent amount of fermentedslurry flows out at outlet. Dome is a drum constructed of mild steel sheets, cylindrical in shape with conical top radial support and fit into digester. As gas is generated, gas holder (dome) rises and float on slurry.

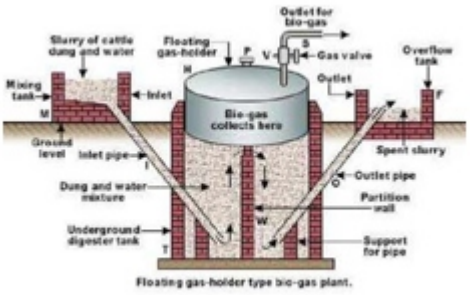

Fig. 5 Floating Biogas unit

A pipe is provided at top of dome for gas collection. A central guide pipe is present to prevent the holder from tilting. The gas escape out passed through soda lime to make it dry.

2. Fixed Dome type biogas plant: It consists of well shaped like underground tank made of bricks and cement called digestive tank provided with inlet and outlet valves. The roof of tank is dome shaped. A gas outlet is provided at top for collection as shown in figure 6. There is mixing tankabove ground levels which is connected to inlet valve of digester through slanting inlet chamber. The outlet chamber is connected to overflow tank which collect used slurry. When animal dung is mixed with water to make slurry and carried to digester tank [10]. The slurry is left for two months for fermentation by aerobic microorganism which produces biogas and collects in dome. It exerts a large pressure on slurry and forced to go in overflow chamber. The biogas is collected through a pipe and used for cooking. There are some difference between floating and fixed dome [11] unit as in Table 3

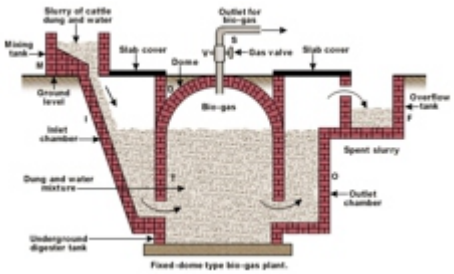

Fig. 6 Fixed Dome Unit

Table 3: Difference between floating and Fixed Dome:

Floating	Fixed Dome
1. Drum consists of masonry digester with steel, plastic or gas holder.	1. It consists of masonry of concrete structure.
2. High cost.	2. Low cost
3. Require more maintenance.	3. Require less maintenance.
4. More reliable	4. Low reliability.
5. Does not require high supervisory skill.	5. Require high supervisory skill.
6. Life span is short.	6. Life span is longer than floating type.
7. Gas pressure remains constant about 10 cm of water.	7.Gas pressure varies between 0-90 cm of water

3. Chinese Type Biogas Plant: Its design consists of fixed dome for collection of gas. Its cost is very much low and construction is quite easier. For construction of 2 m^3 of Chinese plant, its cost just Rs. 2500/- but for KVIC Cost around 5500/-.So, it replaces the floating drum of KVIC digester. A view of Chinese biogas unit is shown as in figure 7.

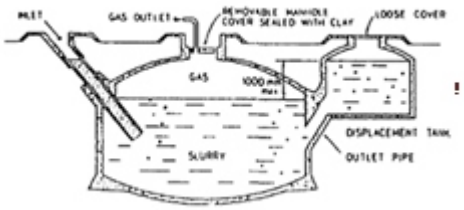

Fig. 7 Chinese Biogas Unit

4. Deenbandhu type plant: Another most popular biogas plant is Deenbandhu model. It has a hemispherical fixed dome type. The dome is made of reinforced concrete and attached to the digester. After fermentation under anaerobic condition, gas is collected at top of dome while sludge comes out through an opening inside of digester. Its cost is much less than KVIC or Chinese type.

Conclusion

Biogas plays an important role to act as renewable energy and assume to be best substitute for use of fossil fuels. The increasing interest in biomass energy and biofuels has wide benefits [12] such as reduction in green house gas emission, substitute for diminishing oil supply, convert waste into energy and energy security. Biomass delivers most energy for domestic use in rural area (approx.90%). Wood fuel contributes 56% of total biomass energy and consumption of wood has grown annually at 2 percent rate over the past two decades. Biomass from agro-waste is available during harvesting season, so there is need to save our desired quantity of biomass in harvesting months. Government should have to adapt policy to use biomass with high potential benefits. These technologies solve many environmental issues especially global warming and sustainable development among poor countries. These not only act as substitute for energy but provide employment opportunity.

Reference

[1] Malik, P. (2014) Solar green house. International Journal of research in Engineering & Applied Science Vol 4(3)
[2] Frisch, L.E (1993) Reliable cogeneration utilizing wood as primary fuel. Paper presented at ASME Power Conference.
[3] Delgado, M. Guariola, E. Biegeniego, M. (1992) Methane generation from water hyacinth biomass.Journal of Environmental Science and health.Vol.27(2)
[4] Nahar,K. (2013) Sustainable biogas from water Hyacinth. The daily star, Environment
[5] Marsh,G. (2009) Biomass from algae. Renewable energy focus
[6] Alder, PR. Sanderson MA, Weimer PJ, Vogel KP. (2009) Plant species composition and biofuel yield of conservation grassland.Ecologicalapplication Vol 19(2)
[7] www.Biomassenergycentre
[8] Basic information on Biogas.www.Kolumbis.fi.Retrieved 2.11.07
[9] Rai. G.D (1997) Solar energy utilization. 5th Ed. Khanna Publishers
[10] www.energypedia.org
[11] Klass, D.L. (2006) Biomass for renewable energy. Fuels and chemicals
[12] NIR Board, (2004) Handbook on Biogas and its application. National Institute of Industrial Research, New Delhi

Solar Powered Air Conditioner

Vijay chauhan*

*Department of mechanical engineering,college of engineering roorkee ,india

ABSTRACT

This paper presents the design of 0.5 tonnes solar air conditoner. The design of energy systems becomes more important due to limitations of fossil fuels and the environmental impact during their use. Energy systems are complex as they involve in economic, technical and environmental factors. The continuous increase in the cost and demand for energy has led to more research and development to utilize available energy resources efficiently by minimizing waste energy. Absorption refrigeration systems increasingly attract research interests.Absorption cooling offers the possibility of using heat to provide cooling. The objective of this paper is to design and study an environment friendly vapour absorption refrigeration system of half unit capacity using R 717 (NH3) and water as the working fluids. The system is designed and tested for various operating conditions using hot water as heat source. The basic idea of this paper is derived from the solar water heating panel installed on the hostel roofs of the institute.

Keywords-soar air conditioner,energy,working fluids.

1. Introduction

solar energy is a very large, inexhaustible source of energy. The power from the sun intercepted by the earth is approximately 1.8 ×1011 MW which is much more larger than the present consumption rate on the earth of all commercial energy sources. Thus, in principle, solar energy could supply all the present and future energy needs of the world on the continuing basis. This makes it one of the most promising of the unconventional energy sources. In addition to its size, solar energy has two other factors in its favor. First unlike fossil fuels and nuclear power, it is an environmental clean source of energy. Second, it is free and available in adequate quantities in almost all parts of the world where people live. However, there are many problems associated with its use. The main problem is that it is a dilute source of energy Refrigeration is the process of removing heat from an enclosed space, or from a substance, and moving it to a place where it is unobjectionable. The primary purpose of refrigeration is lowering the temperature of the enclosed space or substance and then maintaining that lower temperature. The term cooling refers generally to any natural or artificial process by which heat is dissipated. Cold is the absence of heat, hence in order to decrease a temperature, one "removes heat", rather than "adding cold.". In view of shortage of energy production and fast increasing energy consumption, there is a need to minimize the use of energy and conserve it in all possible ways. Energy conservation (i.e.,

energy saved is more desirable than energy produced) is becoming a slogan of the present decade and new methods to save energy, otherwise being wasted, are being explored. Recovering energy from waste heat and/or utilizing it for system efficiency improvement is fast becoming a com-mon scientific temper and industrial practice now days. The present energy crisis has forced the scientists and engineers all over the world to adopt energy conservation measures in various industries. Reduction of the electric power and thermal energy consumption are not only desirable but unavoidable inview of fast and competitive industrial growth throughout the world.

Refrigeration

Refrigeration systems form a vital component for the industrial growth and affect the energy problems of the country at large. Therefore, it is desirable to provide a base for energy conservation and energy recovery from Vapour Absorption System. Although, the investigations undertaken in this work are of applied research nature but certainly can create a base for further R & D activities in the direction of energy conservation and heat recovery options for refrigeration systems and the analysis can be extended further to other refrigeration and Air Conditioning Systems. In recent years,research has been devoted to improvement of Absorption Refrigeration Systems (ARSs). Refrigeration requires high grade energy for their operation.

Apart from this, recent studies have shown that the conven-tional working fluids of vapour compression system are causing ozone layer depletion and green house effect.

Mathematical Modelling

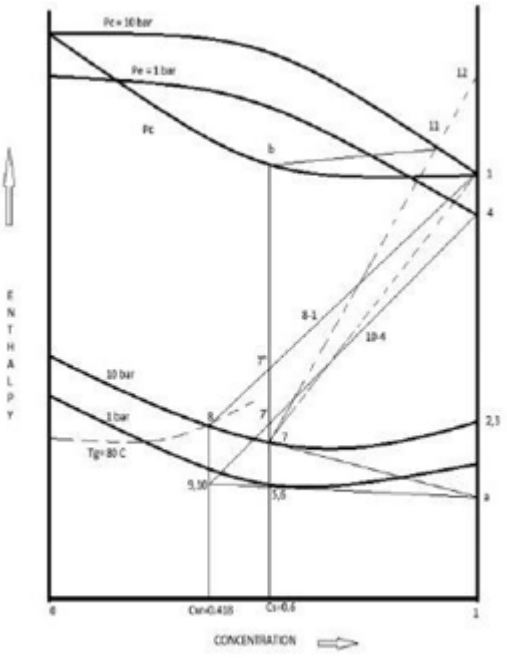

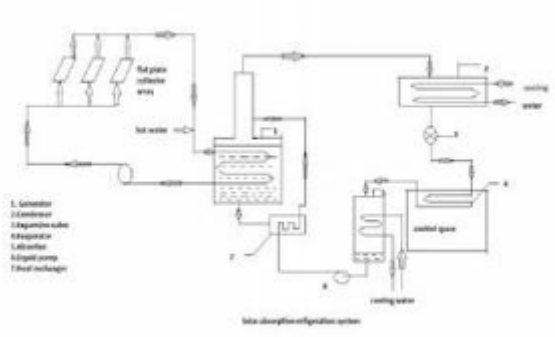

The operating pressures at which the system is working needs to be determined to carry on further calculations, using an enthalpy concentration chart. Once the pressure of the condenser (Pc) and the pressure of the evaporator (Pe) are determined the corresponding points can be fixedon the chart as shown in fig. The various other points and condition lines for components like absorber, generator, heat exchangers etc can be subsequently fixed.

A. Condenser Pressure (Pc) The pressure to be maintained in the condenser for changing the phase of ammonia vapours into ammonia liquid depends on type of condensing medium used and its temperature. In this system, water is used as a condensing medium. Water is available at a temperature of 25 ^{0}C. i.e. condensing temperature is Tc= 25 ^{0}C. For condensing ammonia vapours at 25^{0}C, the corresponding pressure required can be noted from the refrigeration table of ammonia (R-717). In this way, the condenser pressure is fixed at Pc=10 bar. B. Evaporator pressure (Pe) The evaporator pressure can be fixed according to the minimum temperature required to be maintained in the evaporator chamber. The pressure maintained in the evaporator should be as close to the atmospheric pressure as possible, because maintaining a higher pressure is a difficult and costly affair. Moreover it also has leakage problems and the unit needs to be hermetically sealed. The evaporator pressure is kept equal to the atmospheric pressure(1 bar) , to ensure design economy .The corresponding saturation temperature in the evaporator (ammonia vapours) becomes -33 ^{0}C. Now the points of condenser pressure and evaporator pressure can be plotted on the pressure enthalpy chart as points 1, 2, 3 and 4. Point 1 represents pure NH3 saturated vapour at condenser pressure Pc and concentration C=1.

Point 2 represents pure NH3 saturated liq id at Pc and C=1. This point is marked in liquid region. Point 3 represents the condition of pure NH3 (wet) but at pressure Pe and C=1. Point 2 coincides with point 3 as 2-3 is a throttling process in which enthalpy remains contant.

Point 4 represents the condition of pure NH3 at pressure Pe these are saturated vapours which absorbs heat in evaporator and converts from wet vapour to saturated vapour. This point is marked in vapour region. The enthalpies at points 1, 2, 3 and 4 can be noted from the chart.

h1= 1630 KJ/Kg,h2= h3= 460 KJ/Kg, h4= 1530 KJ/Kg

Now, let as assume the refrigeration capacity of the unit to be 0.5TR.

1. The refrigerating effect produced or the heat absorbed by ammonia refrigerant in the evaporator is Qe= h4 – h3 KJ/Kg of ammonia Say the mass flow rate of ammonia in the evaporator be Mr.

Therefore,

Mr × (h4 – h3) = 1 TR

Mr × (h4 – h3) = 105 KJ/min

Therefore,Mr × (1630 - 460) = 210

It gives Mr = 0.09 Kg/min

Thus the mass flow rate of the ammonia through the evaporator ie

Mr = 0.09 Kg/min

2. Now, the temp. of the water going inside the generator is more than 800C (about 84 0C) . That is, taking the temp. in the generator Tg = 80 0C (assuming losses)

Thus the point 8 can be marked on the pressure enthalpy chart where the constant temp line of 80 0C intersects the pressure line of 10 bar.

Point 8 represents the hot weak liquid having concentration Cw inside the generator.

Thus the corresponding concentration of the weak solution can be directly noted down from the chart as Cw = 0.418 After fixing the point 8, the point 5 can also fixed,

Point 5 represents the strong aqua coming out of the absorber after absorbing the vapours coming out of the evaporator. The concentration of the strong solution, say C5, can be determined by knowing the degasifying factor.

The degasifying factor is the amount of NH3 vapours removed from the strong solution in the generator. Higher value of this factor is desirable because its higher value prevents water from being evaporated, which creates trouble, and is necessary to be removed before entering into condenser.

Here in this system, a mass of 0.09 Kg/min is required to be flown across the evaporator for steady state.

Thus the degasifying factor becomes 0..09

Thus the concentration of strong aqua solution becomes
C5= Cw + 0.18
i.e., C5= .418 + .09 = 0.508

Thus taking the concentration of strong solution to be Cs= C5= 0.6

Hence now we know the concentration and pressure at point 5, thus point 5 can be located on the chart at C5= 0.6 and pressure Pc = 10 bar.

Point 6: This is the condition of the aqua solution whose concentration C5 = 0.6, but the pressure is increased from Pe to Pc as it passes through the pump. Point 6 coincides with point 5 on the C-h chart as enthalpy does not change when the aqua pressure increase passing through the pump.

Point 7: As the strong low temperature aqua solution passes through heat exchanger it gains the heat and its enthalpy increases, but its concentration Cs remains same as well as pressure remains same as Pc. Now the point 7 can be marked on the C-h diagram as pressure at 7 and C7 are known.

Now join points 8 and 7 and extend till it cuts the Y axis (enthalpy) at „a" as shown in figure, then join point „a" and 5 and extend till it cuts the vertical line passing through 8.

This also decides the position of point 9 and 10.

Point 9: This shows the condition of weak liquid coming out of the heat exchanger after giving heat to the strong solution. So enthalpy is reduced. Subtracting the heat lost by the weak solution in heat exchanger, point 9 can be marked as the concentration does not change.

Point 10: The point 10 represents the same enthalpy as 9 but at reduced pressure Pe as it passes through the pressure reducing valve.

Absorber

In absorber, the pure NH3 gas enters at condition 4 and weak aqua solution enters at condition 10 and after mixing, strong aqua comes out at condition 5. The mixing occurring inside is underlined but aqua condition coming out is definitely known. Join the points 10 and 4 and extend the vertical line passing

through point 7 till it cuts at point 7". Now we can say that mixing taking place along the line 4- 10 and at pressure Pe and resulting aqua is coming out at 5 after losing heat in the absorber. Joining the points 4 and 10 and marking point 7" is not necessary for solving problems or designing the system components.

Generator(solar collector tubes)

In generator, strong aqua is heated by supplying heat Qg,.

The strong aqua enters into the generator at condition 7 and pure NH3 vapour comes out at condition 1 and weak aqua at condition 8. Now join the points 8 and 1 and extend the vertical line through point 7 to mark the point 7" which cuts the line 1-8. Now, we can say that the separation is taking place along the line 1-8 and at pressure pc. Joining the points 1 and 8 marking the point 7" is not necessary for solving the problems or designing the system components.

IV. Calculations:

a) Mass flow rate of ammonia as refrigerant

Mr = 0.09 Kg/min

b) removed in the evaporator

= refrigeration effect

= Mr. × (h4 – h3)

= 0.5 TR = 105 KJ/min

If cold water flow rate is Mw then

Mw Cp ΔT= 105 Kj/min, if ΔT=17 ^{0}C

then Mw= 3.0 Kg/min

c) Heat removed in condenser

Heat removed in the condenser by the circulated cooling water is given by the equation:

Qc = (h4-h3) per kg of ammonia

i.e. Qc = Mr × (h2 – h1)

= 0.09 × (1630 - 460)

Therefore, heat removed Qc = 105.8 KJ/min

d) Heat removed from absorber.

When the NH3 vapour at point 4 and aqua at 10 are mixed, the resulting condition of the mixture in the absorber is represented by 7" and after losing the heat in the absorber (as it is cooled), the aqua comes out at condition 5. Therefore, the heat removed in the absorber is given by

Qa = (h7" – h5) per Kg of aqua.

Extend the triangle 10-7"-5 towards right till 10-7" cutsat 4 and 10-5 cuts at point „a" on x axis.

Therefore, heat removed per kg of NH3 is given by Qa = (h4 - ha) per kg of ammonia

Qa = Mr × (h4 - ha)

= 0.09 × (1550 - 70)

= 133.2 KJ/ min Thus Qa = 133.2 KJ/min

c cuts at 1 and 8-7 cuts at a on y axis, then the heat removed per kg of NH3 is given by

g - Qd = (h1 – ha) per kg of ammonia

Now for finding out Qd separately, extend the vertical line 7-7" till it cuts the auxiliary line Pc and mark point „b" as shown. Then draw a horizontal line through b which cuts Pc line in vapour region at point 11. Then join the points 7 and 11 and extend the line till it cuts y axis at 12.

Then Qd is given by Qd = (h12 – h1) per kg of ammonia

Qd = 0.09 × (1760 - 630)

Qd = 101.7 KJ/min

now using equation Qg – Qd = (h1 - ha) we have Qg - 23.4 = .09 × (1630 - 70)

therefore, Qg = 140.4 KJ/min

Thus the amount of heat required in the generator for running this unit is

Qg = 152.1 KJ/min. The temp of hot water coming out of evacuated solar tube collector is about 84 ^{0}C. We can reasonably assume that the heating in generator is produced at about 80 ^{0}C, considering losses of heat.

e). Heat given in the generator

Say Qg is the heat supplied in the generator and Qd is the heat removed from water vapour then the net heat removed per kg of aqua is given by

qg – qd = (h7‟ – h7) per kg of aqua

as the aqua goes out in at condition 7 and comes out at condition 8 and 1, which can be considered as a combined condition 7‟.By extending the triangle 8-7-7‟ towards right till 8-7‟ Let rate of water flowing through the tubes ,

m = 1.2 kg/min = 0.02 kg/s, (typical example) Specific heat of water, Cp=4200 J/kg/k To=Outlet temp. of water in the collector plate

Ti=Inlet temp. of water in evacuated solar tube collector=25 ^{0}C

Therefore, Qu = 0.02 × 4200 × (To-25) i.e. 0.02 × 4200 × (To - 25) = 5070

It gives, To = 84 ^{0}C

The temperature (To) should be the inlet temp. of generator, but assuming water loses heat while flowing through the tubes. Also there is certain effectiveness of the generator as a heat exchanger, less that 100 %. Hence net heating in the generator can be assumed to be taking place at 80 ^{0}C

Temperature at generator=80 0C

This is the net heat input to the system, which is running as a refrigeration unit of 0 .5 TR capacity.

The work done by the pump for raising the pressure is negligible and hence neglected.

g. COP Of The System

The cop of the refrigerating unit can be calculated by using the equation:

$$COP = \frac{\text{Refrigeration effect}}{\text{Heat input in generator}}$$

$$\text{i.e. } COP = \frac{Q_e}{Q_g}$$

Neglecting pump work

Therefore, COP = 105 / 152.1 = 0.69

performance is also calculated. The results can be summarized as:

- Mass flow rate of cold water=3 Kg/min Designed operating conditions:
- Condenser pressure: 10 bar
- Evaporator pressure: 1 bar
- Heat input required (at generator) = 152.1 KJ/min
- Output temp of water from evacuated tube solar collector = 84 0C
- COP of refrigerating unit = 0.69

In light of the above results, the feasibility of the solar powered vapour refrigeration system has been reasonably proved. The COP values as calculated by us are on a little higher side than the actual COP"s, but , because we have assumed ideal processes in heat exchanges etc, this obliquity can be understood.

Hence, an air conditioning unit can be usefully employed during summer conditions.

V. Results And Conclusions

We have used 3 evacuated solar tube collector for the refrigeration unit,the calculations are as shown below

Vol. of 3 tube =0.0087m^3

Angle of tubes with ground = 12

Heat gained Q = 0.404 kJ/sec η = 81%

Required Q in generation for .5 TR = 2.53kj/sec Required area = 2.53/.465=5.44m²

Number of tube ≈ 56 tubes

Mass flow rate of ammonia (Mr)=.09kg/min Heat removed in the condenser= 105.3kj/min Heat removed in absorber = 133.2 kw/min Mw=.5788kg/min

Heat supplied in generator (Qg)=152.1kj/min COP of refrigeration unit .69

So we would require about 56 solar collector tubes (as shown in figure) for refrigeration capacity of 0.5 tonnes.

References

[1] B.H. JENSLINGS, and P.L. BLACKSHEAR, "Tables of specific volume of aqua ammonia solutions",ASHRAE Handbook, pp.187. 1951.W.-K. Chen, Linear Networks and Systems (Book style). Belmont, CA: Wadsworth, 1993, pp. 123–135.
[2]V.F. TCHAIKOVSKY. And A.P. KUTEZSOV, "Utilisation of refrigerant mixtures in refrigerating compression machinery", Air Conditioning And Refrigeration in india. Vol.4,1964.
[3]R.K. SWARTMAN, and H.A., V.H. , "Performance of a solar refrigeration system using ammonia –sodium thiocyanate", 72- WA/Sol.-3, an ASME publication.
[4]HELLER and FARAGO , "Proceeding of the eighth international congress of refrigerating engineers".
[5]N.R. SPARKS and C.C. DILLIO, "Mechanical refrigeration", Mcgraw-Hill Book Co.Inc. pp. 140-64,1959.
"Refrigeration air conditioning data book design volume", ASRE , pp.5-12to 15,1957.
"thermodynamics properties of ammonia – water solution extended to higher temperature and pressure", ASHRAE Trans., vol. 70, 1964. [7]W.F. STOECKER , "Refrigeration and air conditioning", Mcgraw – hill book co.,Inc. pp. 179-83,1958.
[8] 8. Parabolic trough calculator http://wims.unice.fr/wims/wims.cgi?module=tool/geometry/paratrough [9.] Solar equipment suppliers, http://wims.unice.fr/xiao/solar/equipments-en.html
[10] http://www.cora.nwra.com/~werne/eos/text/nmsea.html [11]. http://www.sudarshansaur.com/
[12.]www.iaeng.org/publication/WCE2012/WCE2012_pp2016-2020.pdf

The Effect Of 27-Day Solar Rotation On Earth Magnetosphere

Sham Singh[1*], A. C. Panday[2], C. M. Tiwari[2], A. P. Mishra[2]

[1]Department of Applied Sciences, Chandigarh Engineering College, Landran, Mohali Punjab

[2]Department of Physics, A. P. S. University, Rewa (M.P) 486003 India

*e-mail: shamrathore@yahoo.com

ABSTRACT

In this paper we present the results of an investigation of the sequence of events from the Sun to the Earth that ultimately led to the geomagnetic activity. We observed from that the good correlation between geomagnetic index Dst and B x V has been observed to be 0.77. The long-term variation of 27 day has shown average correlation between interplanetary and geomagnetic parameters for cycles 22, 23 and 24. The correlation coefficient between solar wind speed with geomagnetic indices Kp, Ap and Dst for the cycles 22, 23 and 24 is found to be 0.69, 0.65 and 0.57 respectively. The origins and outcome of life on Earth are intimately connected to the way the Earth responds to the Sun's variations. The solar activity and the space magnetic storms affect in various ways earth's magnetosphere. Solar conditions are constructive for the progress of electromagnetic disturbances in geospace, which can effectively influence the performance and reliability of space and ground-based technological systems. As the sphere of the human environment and exploration continues to expand towards space, understanding the effects of our active Sun, becomes day after day more important. This paper studied present understanding of the dynamics of the solar- terrestrial environment and its impacts on the earth's magnetosphere.

Key Words: Sunspot Number, Solar Wind Plasma, Total Average Magnetic field B and Geomagnetic stroms.

1. Introduction

Geomagnetic activity variations are observed with the 27-day solar rotation period, however, there have been very few studies on the relative contributions on the 27 day variation. In this section we have tried to obtain more physical insight into these issues by analyzing geomagnetic data over more than a solar cycle with interplanetary parameters. Changes in solar EUV radiation are produced by the non uniform distribution and motion of EUV radiation sources, such as active regions; over the Sun surface as well as the random fluctuation of radiation intensity. As the Sun rotates with a quasi-27 day period, the solar EUV flux measured at 1 AU shows a variation with a broad spectral peak between about 22 and 32 days (Pap et al., 1990; Kane et al., 2001; Kane, 2002, Woods et al., 2005; Ma et al., 2007). Similarly, there are also quasi-27 day variations in solar wind and interplanetary magnetic field (IMF) as solar active regions near solar maximum and corotating interaction regions (CIRs) near

solar minimum rotate with the Sun. The lifetime of solar active regions and CIRs can last longer than one solar rotation period. These recurrent variations have been noticed in solar wind and IMF produce periodic geomagnetic activity of 27-days when solar wind and IMF interact with the magnetosphere (Schreiber, 1998; Parker, 2005, Ma et al., 2012).

Solar plasma disturbance originating on the Sun, such as coronal mass ejection (CMEs), is major factor in determining disturbance in the near-Earth environment. Large scale solar coronal mass ejection (CMEs) travels through the inner heliosphere at the speed of up to 1000 Km/s, reaching the space environment of Earth within one to three days and carrying with them to the potential for major geomagnetic disturbance (Hundhausen et al. 1997; Gosling et al. 1990 and Singh et al. 2012). Coronal mass ejections release huge quantities of matter above the surfaces of the sun near the corona and emission of electromagnetic radiation does refer to the solar flare. The ejected plasma consists of primarily electrons and protons, but may contain small quantities of heavier elements such as helium, oxygen and iron. It is associated with enormous changes and disturbances in the coronal magnetic field. When the ejection is directed towards the Earth and reaches it as an interplanetary coronal mass ejection (ICME), the shock wave of the travelling mass of solar energetic particles causes a geomagnetic storm that may disrupt the Earth's magnetosphere, compressing it on the day side and ending the night side magnetic tail. When the magnetosphere reconnects in the nightside, it creats power on the order of terawatt scale, which directed back towards the Earth's upper atmosphere. Solar activity comprising sunspots and other phenomena is strongly related to the disturbance in the Earth's magnetic field, giving rise to various effects in the Earth's upper atmosphere [Muscheler et al. 2007; Usoskin et al. 2009, Gopalswamy et al. 2010;]. Shocks occur in the solar atmosphere (the corona) during solar flares and other manifestations of solar activity. Flares and coronal mass ejections can inject energy and material into the solar wind driving travelling interplanetary shocks which propagate out through the solar system. The solar wind has high speed and low speed streams, coming from different source regions on the sun. Shocks can form at the interface between a slow stream being overtaken by a fast stream. In more exotic astrophysical bodies one finds jets of material from active galactic nuclei (AGN), and there are probably shocks formed at the interface between the jet material and the interstellar medium. In supernovae massive amounts of energy are deposited in a very short time and shocks are formed as the supernova remnant (SNR) loads up material as it expands away from the newly formed pulsar. In fact' the interplanetary magnetic field is the extension of solar magnetic fields which could not be held static due to the tremendous energy of the solar corona and comes out along with the solar wind in the form of frozen in spiral magnetic lines of force. The high speed solar plasma interacts with Earth magnetic field and creates disturbance in the magnetosphere. Injection of the solar wind energy into magnetosphere produces variations of geomagnetic field at Earth. The IMF

is a weak field, varying in strength near the Earth from 1 to 37 nT, with an average value of ~6 nT. The IMF is the term for the solar magnetic field carried by the solar wind among the planets of the solar system. When the IMF and geomagnetic field lines are oriented opposite or antipallel to each other, they can merge or reconnet resulting in the transfer of energy, mass, and momentum from the solar wind flow to magnetosphere. The strongest coupling with the most dramatic magnetospheric effects occurs when the Bz component is oriented southward. Disturbances created by solar plasma and field sometimes become responsible for adverse effects on satellites, communications, electric power and pipelines. Numerous severe storms occurred during the maximum phase of the solar activity and are mostly associated with CMEs (Srivastava 2005; Zhang et al. 2006; Singh et al. 2012). Most CME initiation models today are based on the premise that CMEs and flares derive their energy from the coronal magnetic field. The currents that build up in the corona as a result of flux emergence and surface flows slowly evolve to a state where a stable equilibrium is no longer possible. Once this happens, the field erupts. If the eruption is sufficiently strong and the overlying fields not too constraining, plasma is ejected into interplanetary space. If strong magnetic fields exist in the erupted region, then bright, flare-like emissions occur. The latter is true, even if the field does not erupt (Gopalswamy et al 2007)

Several authors have studied the geoeffectiveness of magnetic clouds for longer time intervals (Gosling et al. 1991; Echer et al. 2005) and of other interplanetary structures for several levels of the intensity of magnetic storms, also involving superstorms (Gonzalez et al. 1994, 1999, Srivastava 2005; Zhang et al. 2006; Richardson et al. 2006; Gonzalez et al. 2007 and Singh et al. 2015) Solar energetic transients, i.e. flares and coronal mass ejections (CMEs), occur rather spontaneously, and we have not yet identified unique signatures that would indicate an imminent explosion and its probable onset time, location, and strength.

On the Magnetosphere it has been suspected that “northward turnings” of the solar wind magnetic field can trigger magnetospheric substorms (Rostoker, 1983; Hsu and McPherron, 2006) but see Morley and Freeman (2007) and for evidence against this. These northward turnings occur as solar wind current sheets pass the Earth, and solar wind current sheets typically have co-located velocity shear layers. Hence, sudden wind shear effects may have been hidden in these previous studies of solar wind triggering by sudden magnetic field changes, but the effects of the wind shears were not separately studied. Assessing the separate importance of magnetic field changes and velocity-vector changes on the stability of the magnetosphere should be done. A solar wind discontinuity with the proper orientation can interact with the Earth's bow shock to produce a “hot flow anomaly” (Thomsen et al., 1986; Schwartz et al., 2000) wherein solar wind ions that reflect off the bow shock travel upstream inside the discontinuity and produce a rapid pressure expansion of the discontinuity's

current sheet (Burgess, 1989; Koval et al., 2005]. Hot flow anomalies are known to produce large transient outward displacements of the magnetopause (Borovsky 2012).

2. Selection Criteria And Data Selection

In the present study, we have studied correlation of long-term variation between interplanetary and geomagnetic parameters for cycles 22, 23 and 24. The correlation coefficient between solar wind speed with geomagnetic indices Kp, Ap and Dst for the cycles 22, 23 and 24 were discussed. We have also select the correlation coefficient between Bz-component of IMF with geomagnetic indices Ap, Kp and Dst, and correlation between geomagnetic index Dst and B x V has been analysed.

The relationship between solar activity and geomagnetic indices in solar cycle 22 to 24 has been analysed. The significance of the geomagnetic Ap, Kp index in tracking long-term solar activity has been documented in the literature [8]. For this purpose we have selected data of 27 day values of geomagnetic activity (Kp Indices, Ap Indices and Dst Indices) have been taken from web site (www.geomag.bgs.ac.uk/daaservice/dat). The 27 day variation values of international SSN, Bz-component of interplanetary magnetic field (IMF) and solar wind speed (V) data have been downloaded from the National Geophysical Data Centre web site (htt://www.ngdc.noaa.gov/stp/SOLAR/ftpsunspotnumber.html).

3. Results And Discussion

The effect of geomagnetic activity is very complicated. A large amount of joule heating is deposited at high latitudes during geomagnetically active periods. This causes upwelling of molecular rich air in the auroral region and down welling of atomic rich air at middle and low latitudes and thus changes in thermospheric composition and plasma density (Burns et al., 1991). Geomagnetic storms can also produce penetration electric fields and enhance neutral wind circulation that alters global ionospheric plasma distribution and density (Lei et al., 2008a; Wang et al., 2008, 2010). The relationship of Kp and solar wind speed is clearly seen in (fig. 1). It is observed from (fig. 2, 3 and 4) that the good correlation between total interplanetary magnetic field IMF (B) and geomagnetic index Kp, Ap and Dst has been observed to be 0.74, 0.75 and 0.70 during the cycles 22, 23 and 24 respectively. Positive correlation coefficient has been observed between SSN with geomagnetic indices Kp, Ap, and Dst respectively (fig. 5, 6 and 7).

The long-term variation has shown average correlation between interplanetary and geomagnetic parameters for cycles 22, 23 and 24. The correlation coefficient between solar wind speed with geomagnetic indices Kp, Ap and Dst for the cycles 22, 23 and 24 is found to be 0.69, 0.65 and

0.57 respectively (fig. 8, 9 and 10). We have also obtained the correlation coefficient between Bz-component of IMF with geomagnetic indices Ap, Kp and Dst, positive correlation is found as depicted in fig. 11, 12 and 13. It is observed from (fig. 14) that the good correlation between geomagnetic index Dst and B x V has been observed to be 0.77.

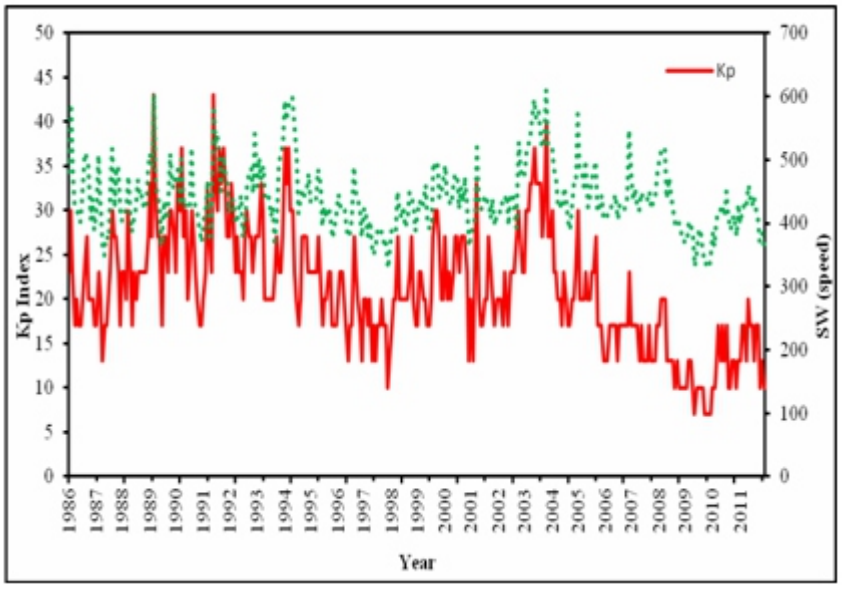

Fig. 1:Shows the relationship between Kp index with interplanetary parameter SW (speed) for 27-day variation during the period 1984 to 2012.

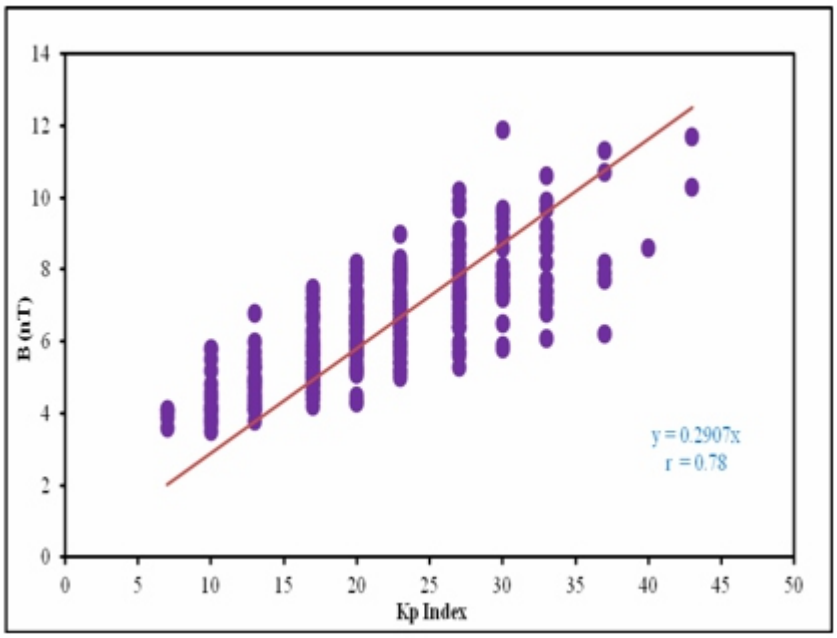

Fig. 2: Shows the correlation coefficient between IMF B(nT) and Kp index for 27-day variation during the period 1986 to 2012.

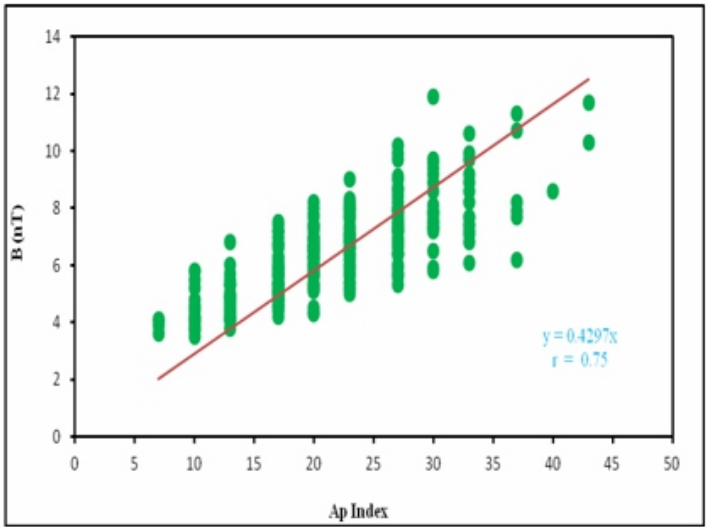

Fig. 3: Shows the correlation coefficient between IMF B(nT) and Ap index for 27-day variation during the period 1986 to 2012.

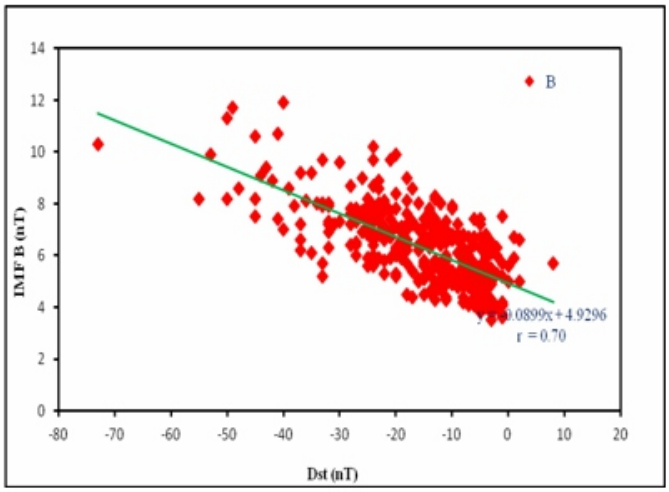

Fig. 4: Shows the correlation coefficient between IMF B(nT) and Dst index for 27-day variation during the period 1986 to 2012.

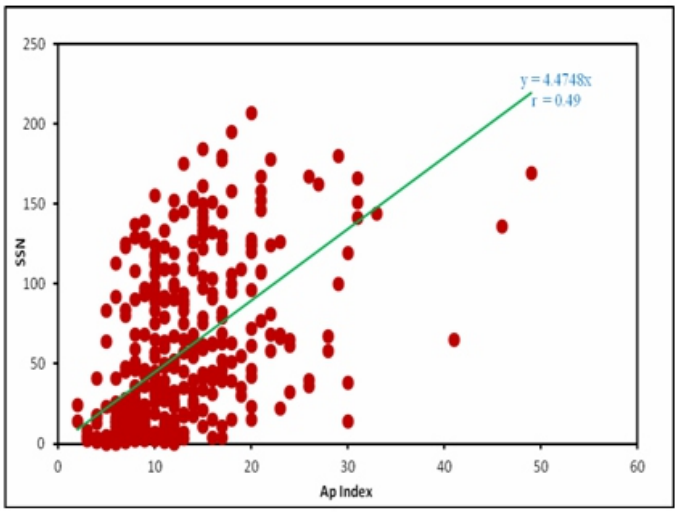

Fig. 5: Shows the correlation coefficient between SSN and Ap index for the 27-day variation during the period 1986 to 2012.

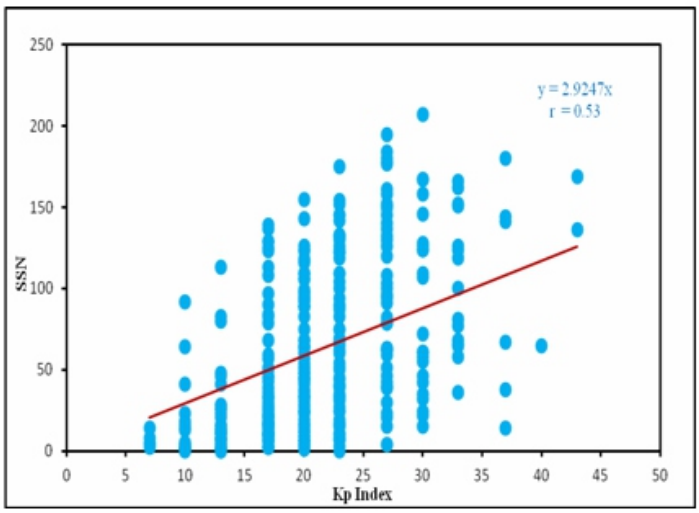

Fig. 6: Shows the correlation coefficient between SSN and Ap index for the 27-day variation during the period 1986 to 2012.

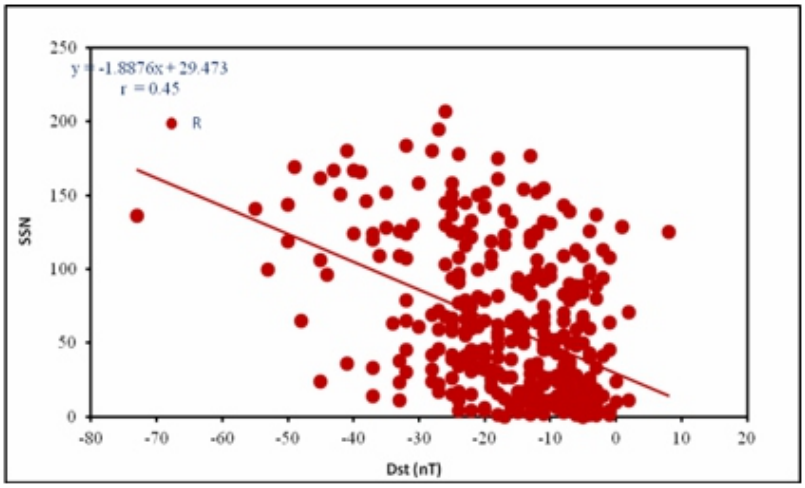

Fig. 7: Shows the correlation coefficient between SSN and Dst index for 27-day variation during the period 1986 to 2012.

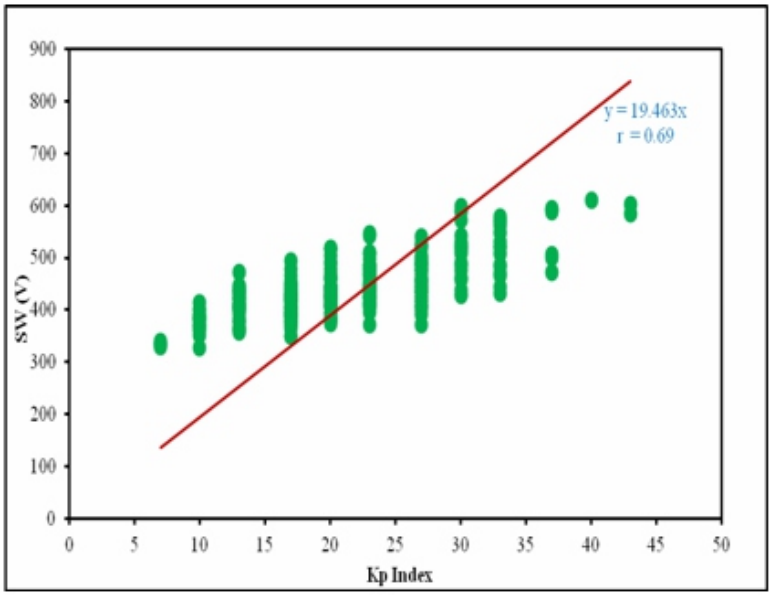

Fig. 8: Shows the correlation coefficient between SW (speed) and Kp index for the 27-day variation during the period 1986 to 2012.

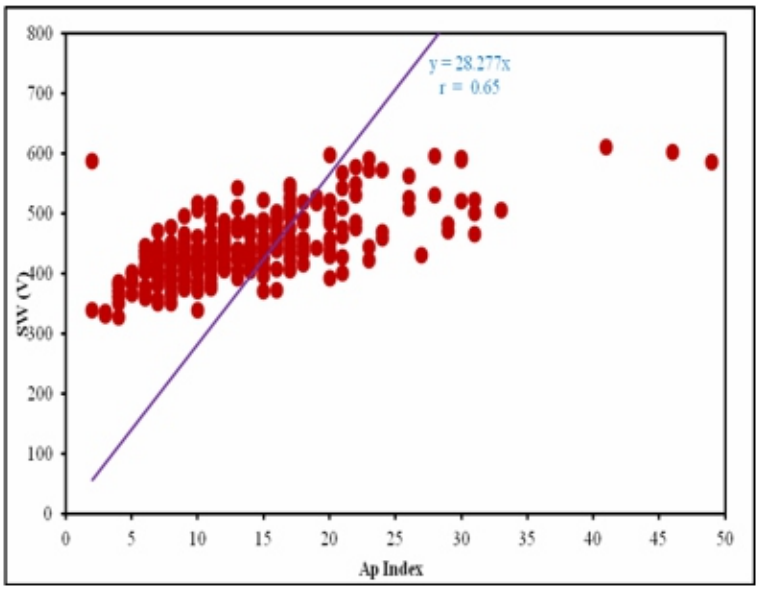

Fig. 9: Shows the correlation coefficientbetween SW (speed) and Ap index for the 27-day variation during the period 1986 to 2012.

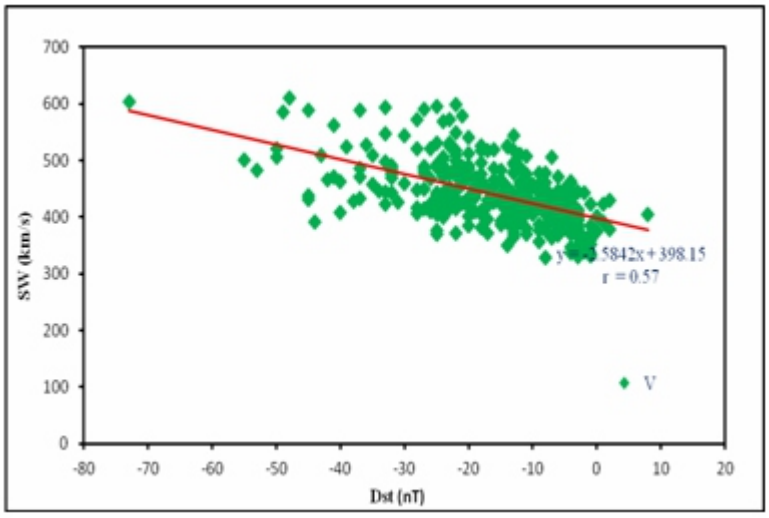

Fig. 10: Shows the correlation coefficient between SW (speed) and Dst index for the 27-day variation during the period 1986 to 2012.

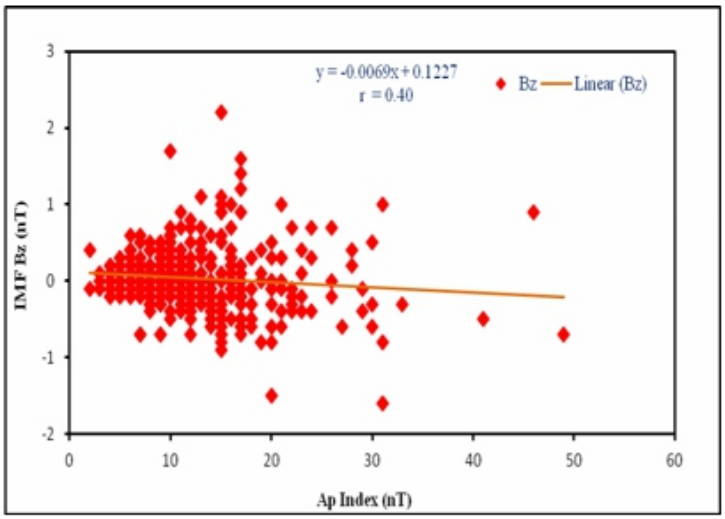

Fig. 11: Shows the correlation coefficient between IMF Bz(nT) and Ap index for 27-day variation during the period 1986 to 2012.

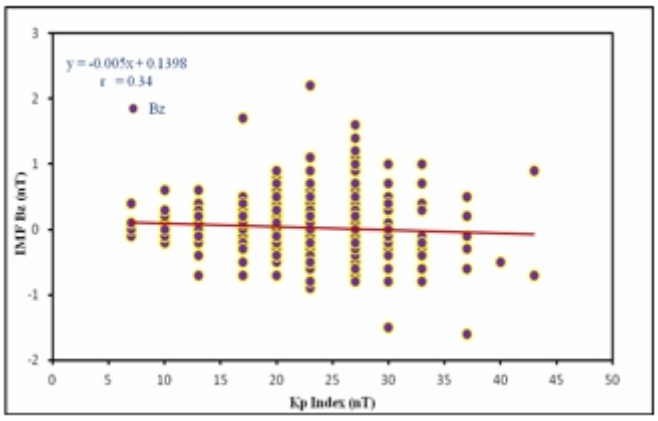

Fig. 12: Shows the correlation coefficient between IMF Bz(nT) and Kp index for 27-day variation during the period 1986 to 2012.

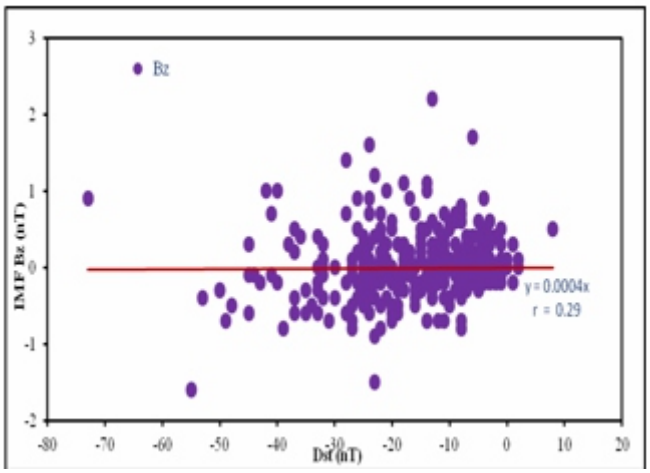

Fig. 13: Shows the correlation coefficient between IMF Bz(nT) and Dst index for 27-day variation during the period1986to 2012.

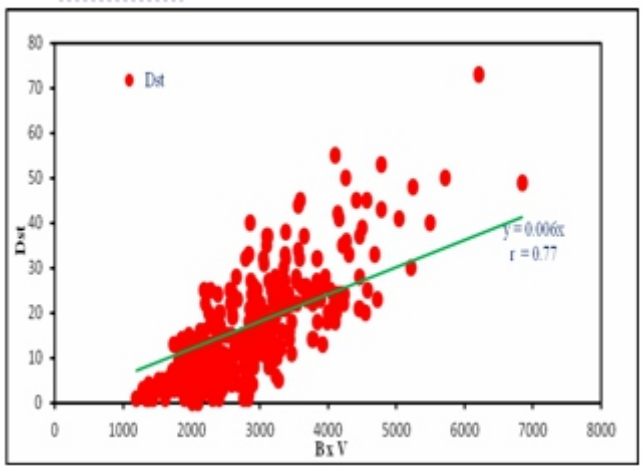

Fig. 14: Shows the correlation coefficient between geomagnetic index Dst and B x V index for 27-day variation during the period1986to 2012.

3 Conclusion

In this paper we considered geomagnetic indices indicate various solar and interplanetary characteristics and their corresponding geomagnetic effects. For each event, peak Dst values as well as date and time of their occurrences has been analysed. Dst decreases with increasing magnetopause shielding currents, a measure of magnetospheric compression produced by an increase in solar wind velocity. Connection between the variation of the solar magnetic field and the solar wind velocity at Earth as determined by the Sun's rotation and dipole tilt and the heliographic location of Earth, geomagnetic activity derived from the time varying geometry of the Sun and Earth was successful in predicting the time variation of the geomagnetic Ap index in selected years. The model accurately predicts the strong semi-annual effect in the ~27 day component of geomagnetic activity, with strongest effect at equinox and with weakest effect at solstice. Thus the expectation is that near equinox the correlation would be higher than the average correlation obtained over the entire year. The variation in geomagnetic activity at this time wouldbe unrelated to solar rotation due to the effect of synoptic weather.

We conclude therefore that, it appears that a significant influence of ~27 day geomagnetic activity on cloud and temperature predictably occurs during years around solar minimum and at times around equinox it would be interesting to examine if this could assist in long term weather prediction. The solar magnetic field and the solar wind velocity contain significant components at harmonics of the 27 day solar rotation period.

4. Acknowledgment

The authors are grateful to Solar Geophysical Data (Prompt Comprehensive report) of U.S. Department of Commerce, NOAA and omni web data for data sets and to the referees for helpful comments.

5. References

[1] A. G. Burns, T. L. Killeen, and R. G. Roble (1991), A theoretical study of thermospheric composition perturbations during an impulsive geomagnetic storm, J. Geophys. Res., 96, 14,153– 14,167.
[2] A. G. Burns, T. L. Killeen, and R. G. Roble. A theoretical study of thermospheric composition perturbations during an impulsive geomagnetic storm, J. Geophys. Res. 1991, 96, 14,153–14,167.
[3] A. Koval, J. Safrankova, and Z. Nemecek (2005), A study of particle flows in hot flow anomalies, Planet. Space Sci., 53, 41, doi:10.1016/j.pss. 2004.09.027.
[4] A Hundhausen, N Crooker, J Joslyn and J Feynman (Eds) American Geophysical Union, Colorado, (1997)
[5] Bame (1986), Hot, diamagnetic cavities upstream from the Earth's bow shock, J. Geophys. Res., 91, 2961, doi:10.1029/JA091iA03p02961.
[6] E. Echer, V.M. Alves, W.D. Gonzalez, A statistical study of magnetic cloud parameters and geoeffectiveness. J. Atmos. Sol.-Terr. Phys. 67, 839–852 (2005)
[7] E. J. Borovsky J. Geophys. Res., 117, A06224, doi:10.1029/2012JA017623, 2012 The effect of sudden wind shear on the Earth's magnetosphere: Statistics of wind shear events and CCMC simulations of magnetotail disconnections

[8] G. D. Parker. "Timing patterns in event lists: Recurrent geomagnetic storms". J. Atmos. Sol. Terr. Phys. 2005, 67.
[9] J Gosling, D McComas, J Phillips, S Bame J. Geophys. Res. 96 7831 (1991).
[10] I Richardson, D Webb, J Zhang, D Berdichevsky, D Biesecker and J Kasper J . Geophys. Res. doi:10.1029/2005JA011476 111 A07S09 (2006)
[11] W Gonzalez, et al J. Geophys. Res. 99 5771 (1994)
[12] G. Rostoker, (1983), Triggering of expansive phase intensifications of magnetospheric substorms by northward turnings of the interplanetary magnetic field, J. Geophys. Res., 88, 6981, doi:10.1029/JA088iA09p06981.
[13] H. Schreiber. On the periodic variations of geomagnetic activity indices Ap and ap, Ann. Geophys. 1998, 16, 510–517.
[14] J. Lei, W. Wang, A. G. Burns, S. C. Solomon, A. D. Richmond, M. Wiltberger, L. P. Goncharenko, A.Coster, and B. W. Reinisch (2008a). "Observations and simulations of the ionospheric and thermospheric response to the December 2006 geomagnetic storm: Initialphase". J. Geophys. Res., 113.
[15] J. E. Borovsky (2012a), The velocity and magnetic-field fluctuations of the solar wind at 1 AU: Statistical analysis of Fourier spectra and correlations with plasma properties, J. Geophys. Res., 117, A05104, doi:10.1029/ 2011JA017499.
[16] J Gosling, S Bame, D McComas and J Phillips, Geophys. Res. Lett. 17 901 (1990)
[17] J Zhang, et al Inter. J. Phys. Astron. 1 1103 (2007) [18] M. F. Thomsen, J. T. Gosling, S. A. Fuselier, and S. J.
[19] R Muscheler, Joos, J Beer, S Muller, M Vonmoos and I Snjwball, Quat Sci. Rev. 26 82 (2007)
[20] N Gopalswamy, et al Geophys. Res. Lett. 27 145 (2000)
[21] N Gopalswamy, S Yashiro and S Akiyama J. Geophys. Res. 112 A06112 (2007)
[22] N. Srivastava, Predicting the occurrenceof superstorms. Ann. Geophys. 23, 2989 (2005)
[23] Pap, J., W. K. Tobiska, and S. D. Bouwer. "Periodicities of solar irradiance and solar activity indices". Sol. Phys. 1990, 129, 165–189.
[24] R Usoskin, K Mursula, R Arlt and G Kovaltsov Astrophys. J. 700 L154 (2009)
[25] R. P. Kane, H. O. Vats, and H. S. Sawant. "Short-term periodicities in the time series of solar radio emissions at different solar altitudes". Sol. Phys., 2001, 201, 181–190.
[26] R. P. Kane. "Some Implications Using the Group Sunspot Number Reconstruction". Solar Phys., 2002, 205, 383-401.
[27] R. Ma. Q. Ji, and J. Xu. "Wavelet analysis of quasi-27-day oscillations in the solar index F10.7". Chin. J. Space Sci., 2007, 27, 89–95.
[28] R. Ma. Xu. Jiyao, W. Wang, and Lei. Jiuhou. "The effect of _27 day solar rotation on ionospheric F2 region peak densities (NmF2)". J. Geophys. Res. 2012, 117, A03303.
[29] S. K. Morley and M. P. Freeman (2007), On the association between northward turnings of the interplanetary magnetic field and substorm onsets, Geophys. Res. Lett., 34, L08104, doi:10.1029/2006GL028891.
[30] S. J. Schwartz, G. Paschmann, N. Sckopke, T. M. Bauer, M. Dunlop, A. N. Fazakeley, and M. F. Thomsen (2000), Conditions for the formation of hot flow anomalies at Earth's bow shock, J. Geophys. Res., 105, 12,639, doi:10.1029/1999JA000320.
[31] S Singh, A Pandey, K Singh and A Mishra Inter. J. Phys. and Astron. 26 1103 (2012)
[32] S. Singh, S. Divya and A.P. Mishra 2012 Effect of solar and interplanetary disturbances on space weather. Indian J.Sci.Res.3(2) : 121-125, 2012
[33] S Singh and A P Mishra 2015 Interaction of solar plasma near-Earth with reference to geomagnetic storms during maxima of solar cycle 24 Indian J Phys DOI 10.1007/s12648-015-0703-y
[34] T. S. Hsu and R. L. McPherron (2006), The statistical characteristics of IMF triggered substorms, in Proceedings of the 8th International Conference on Substorms, edited by M. Syrjasuo and E. Donovan, p. 105, Inst. for Space Res., Calgary, Alberta, Canada. Schreiber, H. (1998), On the periodic variations of geomagnetic activity indices Ap and ap, Ann. Geophys., 16, 510–517.
[35] T. N. Woods, et al. (2005), Solar EUV experiment (SEE): Mission overview and first results, J. Geophys. Res., 110, A01312.
[36] T. N. Woods et al. Solar EUV experiment (SEE): Mission overview and first results, J. Geophys. Res. 2005, 110, A01312.
[37] W Gonzalez, B Tsurutani, and A Clua de Gonzalez Space Sci. Rev. 88 52 (1999).
[37] W. D. Gonzalez, F. L. Guarnieri, A. L. Clua-Gonzalez, E. M. V. Echer, Alves, T. Ogino, and B. T. Tsurutani (2006), Magnetospheric energetic during HILDCAAs, in Recurrent Magnetic Storms: Corotating Solar Wind Streams, Geophys. Monogr. Ser., vol. 167, edited by B. Tsurutani et al., p. 175, AGU, Washington, D. C.

[39]W. Wang, J. Lei, A. G. Burns, M. Wiltberger, A. D. Richmond, S. C. Solomon, T. L. Killeen, E. R. Talaat, and D. N. Anderson. "Ionospheric electric field variations during a geomagnetic storm simulated by a coupled magnetosphere ionosphere thermosphere (CMIT) model". Geophys. Res. Lett. 2008, 35, L18105.
[40] W. Wang, J. Lei, A. G. Burns, S. C. Solomon, M. Wiltberger, J. Xu, Y. Zhang, L. Paxton, and A. Coster (2010). "Ionospheric response to the initial phase of geomagnetic storms: Common features". J. Geophys. Res., 115, A07321.

Determination Of The Effect Of Temperature Changes On Power Output Of Solar Panel

Ilo Frederick .U

Department of Electrical and Electronic Engineering, Faculty of Engineering Enugu State University of Science and Technology (ESUT)

ABSTRACT

It is importance to state that the main limit of photovoltaic power output systems is low conversion efficiency of photovoltaic panels, which is strongly influenced by their operating temperature. Negligence in considering the photovoltaic panel temperature increases the financial risk of system installation. This present study investigates the effects of operating temperature on solar panel power output at Enugu State Nigeria. Experimental approach was adopted in the implementation of the work. Solar panel was positioned outside the Department of Electrical/Electronic Engineering workshop where it will not experience any obstacle from solar radiation intensity. The changes in power output of the solar panel with respect to temperature was measured and recorded. The results show that the power output of the solar panel varies as temperature changes.

Keywords: Photovoltaic, temperature, renewable, Sunlight, Depletion-region

1. Introduction

It is very common in the recent days that people are now seeking for renewable energy in order to replace the current fossil fuels. This is due to the extinction of fossil fuel in the beneath surface of the earth and people cannot depend on it forever. One of the most potential renewable energy found is solar energy (Henry S, 2014). Solar energy is the radiant heat and light from the sun that has been used by humans since ancient times using a wide range of technologies. One of the wide applications of solar energy is photovoltaic (PV). PV is the field of technology and research related to the application of solar cells for energy by converting sunlight directly into electricity by the photovoltaic effect. Solar panels or photovoltaic arrays and solar modules are made by assembling of solar cells. Increasing efforts are directed towards reducing the installation costs and enhancing the performance of photovoltaic systems so that the system can be deployed at a large scale. However, PV solar cells are semiconductor devices which directly convert energy into electricity (Pradhan. A, 2013). Solar cells operate as a quantum device exchanging photons for electrons. Photons from the sun with sufficient energy near the depletion region of a p-n junction produce electron-hole pairs. If these electrons have enough energy, they will move to the conduction band, leaving holes in the valence band. The potential difference across the depletion region provides an electric field that pulls the electron to the n-region and hole to

the p-region (Hart .G and Raghuuraman P, 2010) . The newly free electron can then flow from the n-region to the p-region and recombines with the newly created holes. In this way the energy of the incident photon is converted. The PV solar cells output performance varies with atmospheric factors. Since sunlight is intermittent, solar cells cannot produce energy at a constant rate and the power delivered at a certain instant is still very much a function of climatological factors (Abhishek.k.T and Aruna, 2017).

1.2 How Solar Cell Work

When light shines on solar panel it generated electron-hole pairs across the whole device. If the device is open circuited, the electron hole pairs generated near the depletion region tend to recombine with the charge in the depletion region, thus reducing the depletion region charge and eventually reducing the depletion region. The reduction in depletion region is equivalent of applying a forward bias to the device i.e. this reduction in depletion region tends to develop a potential across the open terminals of the device. The maximum voltage that can be developed is the maximum forward drop across the device which theoretically is possible with the complete elimination of the depletion region (Green. A and Martin, 1982). This maximum voltage that can be developed across the open circuited device is called the open circuit voltage. If the device is short circuited, the generated holes and electrons produce a current corresponding to the incoming photons. This current is called the short circuit current Solar panels work best in certain weather conditions, but since the weather is always changing and as engineers are installing solar panels all over the world in different climate regions, most panels do not operating under ideal conditions. That is why it is important for engineers to understand how panels react to different weather conditions. With this knowledge, they can design ways to improve the efficiency of solar panels that operate in non-optimal conditions. In some cases, they can design cooling systems to keep the panels withincertain temperatures. For example, solar power plants in extremely hot climates may pass a cool liquid behind the panels to pull away heat and keep the panels cool.

1.3 Modeling Of Solar Cell

To understand the electronic behavior of a solar cell, it is useful to create a model which is electrically equivalent whose behavior is well defined. A solar cell was modelled by a current source in parallel with a diode. In practice no solar panel is ideal, so a shunt resistance and a series resistance component are added to the model Krauter. S, 2004. The circuit model of a solar cell is drawn in Figure 1(a)

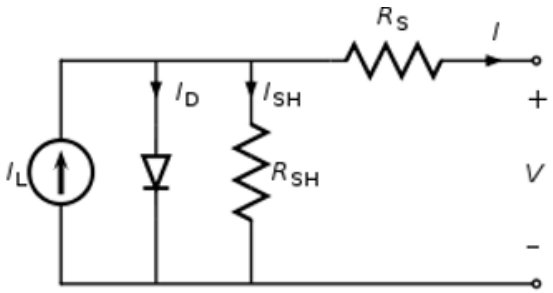

Figure 1(a): Solar cell model

From the circuit model in Figure 1(a), it is evident that the current produced by the solar cell is equal to that produced by the current source, minus that which flows through the diode, minus that which flows through the shunt resistor such that:

$$I = I_L - I_D - I_{SH} \qquad (1)$$

Where

I = output current of a solar panel (ampere)

I_L = photogenerated current (ampere)

I_D = diode current (ampere)

I_{SH} = shunt current (ampere).

The current through the circuit is governed by the voltage across them:

$$V_J = V + IR_S \qquad (2)$$

Where

V_j= voltage across both diode and resistor

R_{SH} (volt)

V = voltage across the output terminals (volt)

I = output current (ampere)

R_S = series resistance (Ω).

From the Shockley diode equation, the current diverted through the diode Ike.C.U, (2013) is

$$I_D = I_o\left\{\exp\left[\frac{V_j}{nV_T}\right] - 1\right\} \qquad (3)$$

where

I_0 = reverse saturation current (ampere)

n = diode ideality factor (1 for an ideal diode)

V_T = KT/q: the thermal voltage. At 25 °C,

From Ohm's law, the current diverted through the shunt resistor is:

$$I_{SH} = \frac{V_j}{R_{SH}} \qquad (4)$$

Substituting equations (2), (3) and (4) into equation (1) produces the characteristic model equation of a solar cell, which relates solar cell parameters to the output current and voltage.

$$I = I_L - I_O\left\{\exp\left|\frac{V + IRs}{nV_T}\right| - 1\right\} - \frac{V + IRs}{R_{SH}} \qquad (5)$$

1.4 Open-Circuit Voltage And Short-Circuit Current

I LWhen solar cell is operated at open circuit, I = 0 and the voltage across the output terminals is defined as the open-circuit voltage. Assuming the shunt resistance is high enough to neglect the final term of the characteristic equation, the open-circuit voltage VOC is:

$$V_{oc} = \frac{nKT}{q}\ln\left|\frac{I_L}{I_o} + 1\right| \qquad (6)$$

Where,

q = charges

k = Boltzmann's constant

T = absolute temperature

Similarly, when solar panel is operated at short circuit, V = 0 and the current I through the terminals is defined as the short-circuit current (Jafari V.F, 2011). It can be shown that for a high-quality solar panel(low R_S and I_0, and high R_{SH}) the short-circuit current ISC is:

$$I_{SC} = I_L \qquad (7)$$

It is not possible to extract any power from solar cell when operating at either open circuit or short circuit conditions.

1.5 Types Of Photovoltaic Solar Cells

The main types of solar cells in use today are crystalline silicon, both single and multi-crystalline, and they are known as thin film solar cells, which include amorphous silicon, cadmium telluride, copper indium gallium diselenide (CIGS), and copper indium diselenide (CIS) Mahfoud .A etal (2015). Organic photovoltaic cells and dye-sensitized cells have been discovered. It is the connection of two or more cells either in series or parallel makes photovoltaic panel.

1.6 Materials And Methods

Experimental method was used to generate the result of these practical results in table 1. Three flat plate photovoltaic solar modules of the same material were used for the study. Each solar module containing seventy two amorphous silicon solar cells, rated 30W peak, 21V, model G100, ARCO. SOLAR INC, active area of 30cm^2 and manufactured by BP solar system LTD. A 6.1kΩ variable resistor was used as a load in the study. A low resistance ammeter, high resistance voltmeter, and five in one Auto Raging Digital Multi-meter (serial number M58209) were used for monitoring and measuring the output current, voltage and ambient temperature, respectively. The product of voltage and current was done to obtain power.

1.7 Experimental Set-Up

The photovoltaic panel includes three flat amorphous silicon solar modules connected in parallel configuration. They were mounted horizontally on a metal plate frame, which was raised above the roof-top using an iron steel pole at the back of the Department of Electrical and Electronic Engineering workshop at Enugu State University of Science and Technology. The photovoltaic solar electricity array was capable of operating in the range of 80W – 100W, 12V – 20V. To the PV solar array, a low resistance voltmeter was connected in series while a high resistance voltmeter was connected in parallel to the 6.1kΩ variable resistor using as a load. Figure 1 shows the circuit model of experimental set-up. Thermometer was used to measure temperature of the photovoltaic panel.

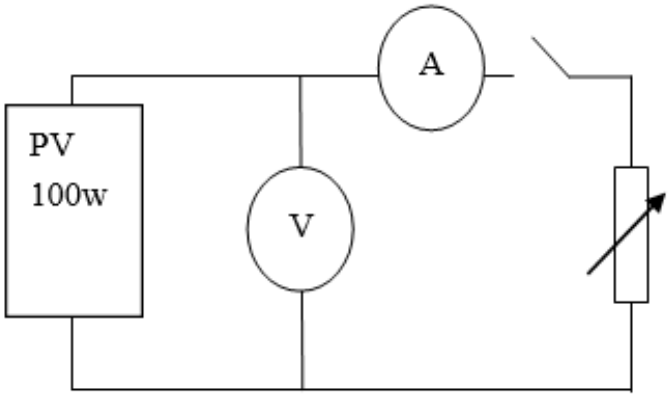

Figure 1: Shows the circuit model of Experimental set-up

Table1: The average monthly values of Temp. And power output of a solar panel for year 2014

MONTHS	Temp. (^{O}C)	PV Power Output(W)
January	34.2	70.2
February	33.1	68.6
March	35	72.1
April	32.4	68.2
May	30.1	67.4
June	29.2	67.2
July	28	66.8
Aug	28.6	67
September	29	67.6
October	30.1	68
November	32	67.8
December	33.2	68.4

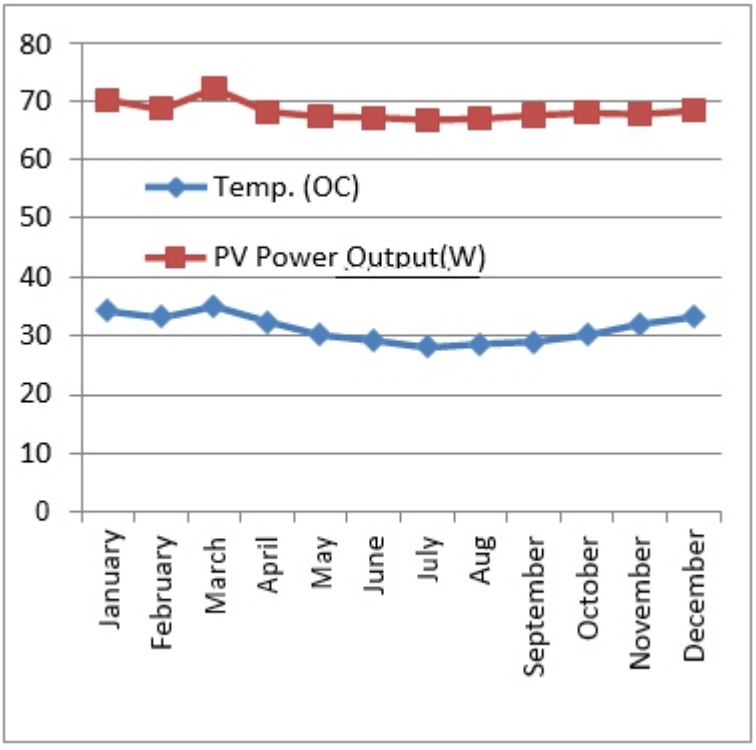

Figure 2: Shows the graph of temp. Vs power output of a solar panel for year 2014

Table2: The average monthly values of Temp. And power output of a solar panel for year 2015

MONTHS	Temp.(^{O}C)	PV Power Output(W)
January	34.3	70
February	33.6	69.4
March	34.6	71.1
April	33.1	68.3
May	32	67.8
June	30.2	67.2
July	29.4	67
Aug	29.6	67.2
September	29	67.4
October	31.2	68.6
November	33.3	69
December	33.6	69.8

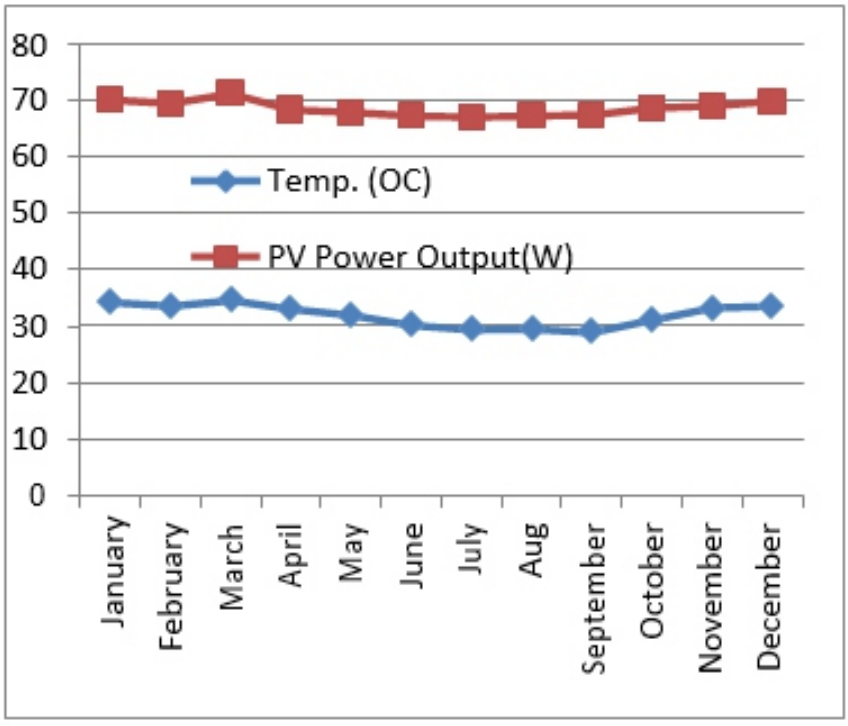

Figure3: Shows the graph of temp. Vs power output of a solar panel for year 2015

Table3: The average monthly values of Temp. And power output of a solar Panel for year 2016

MONTHS	Temp. (^{O}C)	PV Power Output(W)
January	36	73
February	34.2	72.2
March	35.1	72
April	33	71
May	30.8	70.4
June	30.6	70.4
July	29.6	69.8
Aug	28.4	68
September	29.8	68.4
October	30	70.1
November	31.1	70.2
December	32.3	71.4

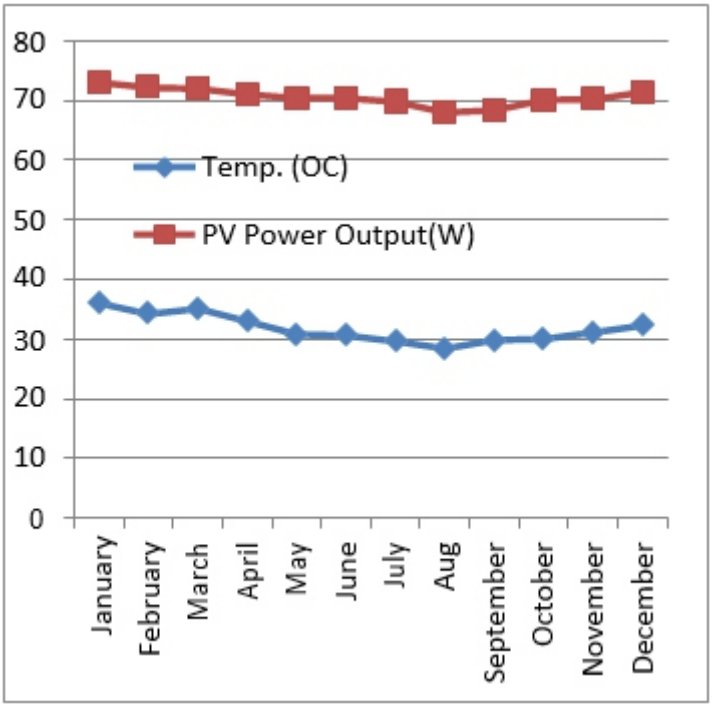

Figure 4: Shows the graph of temp. Vs power output of a solar panel for year 2016

Results Analysis

The results obtained from the experiment were presented in both tabular and graphical forms in other to bring out the detailed results. From Table 1, the monthly values of average Temperature and power output of a solar panel obtained in the year 2014 was presented. In Figure 2, the graph of table 1 was presented. It was observed that the power output of solar panel varies with temperature changes. Again in the year 2014, it was observed that the highest power output of a solar panel recorded was on match

and the value was 72.10W at a temperature of 35°C. Table 2 shows the average monthly values of data obtained in the year 2015. Figure 3 was the graphical representation of table 2. From the results, it was observed that the highest values of power outputs obtained in the year 2015 were in the months of November, December, January, February and March. The maximum values of power output in these months of the year were attributed to the high solar radiation intensity received, a period when the atmosphere is relatively clean and clear, as a result of little or no cloud, dust free and low humidity. Table 3 shows the average monthly values of temperature and power output of a solar panel in the year 2016 while figure 4 shows the graph of table 3. From the results, it is observed that, the power output of a solar panel changes with temperature.

Conclusion

Based on the results obtained, it is clearly shown that Temperature has great effect on the power output of a Solar panel. So it is advisable that when installing Solar panel on a roof, a space of few inches should be provided to allow air flow to cool the panel. Again the manufacture of solar panel should produce it with light cooled material to reduce heat absorption.

Reference

Abhishek.k.T and Aruna (2017): Output power loss of photovoltaic panel due to dust and temperature .International Journal of Renewable Energy Research.

Green. A and Martin (1982): Solar cells: Operating Principles, Technology and system Applications, Prentice-Hall: Englewood cliffs, NJ.

Hart. G and Raghuraman. P (2010): Simulation of thermal aspects of residential Photovoltaic systems, MIT Report.

Henry .S(2014): Maximum Power tracking for photovoltaic power system Development and Experimental comparison of two algorithms. Renewable Energy, Pg 2381-2487.

http://www.pvpowerway.com/en/knowledge/photovoltaic.html.

Ike .C.U (2013): The effect of temperature on the performance of a photovoltaic solar system in Eastern Nigeria. International Journal of Engineering and Science Pg 10-14.

Jafari V.F. (2011): Effect of Temperature on photovoltaic cell efficiency. International Conference on Emerging Trends in Energy conservation-ETEC.

Krauter. S. (2004): Increased electrical yield via water flow over the front of photovoltaic panels. Solar Energy materials and solar cells.

Mahfoud .A, Mekhilef.S and Djahli .F (2015): Effect of Temperature on the GaInP/GaAs Tandem solar cell. International Journal of Renewable Energy Research (IJRER) Pg 629-634.

Pradhan Arjyahara and Ali .S.M (2013): Analysis of solar PV cell performance with changing Irradiance and Temperature. International Journal of Engineering and Computer Science Pg 214-220.

Instructions for Authors

Essentials for Publishing in this Journal

1 Submitted articles should not have been previously published or be currently under consideration for publication elsewhere.

2 Conference papers may only be submitted if the paper has been completely re-written (taken to mean more than 50%) and the author has cleared any necessary permission with the copyright owner if it has been previously copyrighted.

3 All our articles are refereed through a double-blind process.

4 All authors must declare they have read and agreed to the content of the submitted article and must sign a declaration correspond to the originality of the article.

Submission Process

All articles for this journal must be submitted using our online submissions system. http://enrichedpub.com/ . Please use the Submit Your Article link in the Author Service area.

Manuscript Guidelines

The instructions to authors about the article preparation for publication in the Manuscripts are submitted online, through the e-Ur (Electronic editing) system, developed by **Enriched Publications Pvt. Ltd**. The article should contain the abstract with keywords, introduction, body, conclusion, references and the summary in English language (without heading and subheading enumeration). The article length should not exceed 16 pages of A4 paper format.

Title

The title should be informative. It is in both Journal's and author's best interest to use terms suitable. For indexing and word search. If there are no such terms in the title, the author is strongly advised to add a subtitle. The title should be given in English as well. The titles precede the abstract and the summary in an appropriate language.

Letterhead Title

The letterhead title is given at a top of each page for easier identification of article copies in an Electronic form in particular. It contains the author's surname and first name initial .article title, journal title and collation (year, volume, and issue, first and last page). The journal and article titles can be given in a shortened form.

Author's Name

Full name(s) of author(s) should be used. It is advisable to give the middle initial. Names are given in their original form.

Contact Details

The postal address or the e-mail address of the author (usually of the first one if there are more Authors) is given in the footnote at the bottom of the first page.

Type of Articles

Classification of articles is a duty of the editorial staff and is of special importance. Referees and the members of the editorial staff, or section editors, can propose a category, but the editor-in-chief has the sole responsibility for their classification. Journal articles are classified as follows:

Scientific articles:

1. Original scientific paper (giving the previously unpublished results of the author's own research based on management methods).

2. Survey paper (giving an original, detailed and critical view of a research problem or an area to which the author has made a contribution visible through his self-citation);

3. Short or preliminary communication (original management paper of full format but of a smaller extent or of a preliminary character);

4. Scientific critique or forum (discussion on a particular scientific topic, based exclusively on management argumentation) and commentaries. Exceptionally, in particular areas, a scientific paper in the Journal can be in a form of a monograph or a critical edition of scientific data (historical, archival, lexicographic, bibliographic, data survey, etc.) which were unknown or hardly accessible for scientific research.

Professional articles:

1. Professional paper (contribution offering experience useful for improvement of professional practice but not necessarily based on scientific methods);
2. Informative contribution (editorial, commentary, etc.);
3. Review (of a book, software, case study, scientific event, etc.)

Language

The article should be in English. The grammar and style of the article should be of good quality. The systematized text should be without abbreviations (except standard ones). All measurements must be in SI units. The sequence of formulae is denoted in Arabic numerals in parentheses on the right-hand side.

Abstract and Summary

An abstract is a concise informative presentation of the article content for fast and accurate Evaluation of its relevance. It is both in the Editorial Office's and the author's best interest for an abstract to contain terms often used for indexing and article search. The abstract describes the purpose of the study and the methods, outlines the findings and state the conclusions. A 100- to 250- Word abstract should be placed between the title and the keywords with the body text to follow. Besides an abstract are advised to have a summary in English, at the end of the article, after the Reference list. The summary should be structured and long up to 1/10 of the article length (it is more extensive than the abstract).

Keywords

Keywords are terms or phrases showing adequately the article content for indexing and search purposes. They should be allocated heaving in mind widely accepted international sources (index, dictionary or thesaurus), such as the Web of Science keyword list for science in general. The higher their usage frequency is the better. Up to 10 keywords immediately follow the abstract and the summary, in respective languages.

Acknowledgements

The name and the number of the project or programmed within which the article was realized is given in a separate note at the bottom of the first page together with the name of the institution which financially supported the project or programmed.

Tables and Illustrations

All the captions should be in the original language as well as in English, together with the texts in illustrations if possible. Tables are typed in the same style as the text and are denoted by numerals at the top. Photographs and drawings, placed appropriately in the text, should be clear, precise and suitable for reproduction. Drawings should be created in Word or Corel.

Citation in the Text

Citation in the text must be uniform. When citing references in the text, use the reference number set in square brackets from the Reference list at the end of the article.

Footnotes

Footnotes are given at the bottom of the page with the text they refer to. They can contain less relevant details, additional explanations or used sources (e.g. scientific material, manuals). They cannot replace the cited literature.
The article should be accompanied with a cover letter with the information about the author(s): surname, middle initial, first name, and citizen personal number, rank, title, e-mail address, and affiliation address, home address including municipality, phone number in the office and at home (or a mobile phone number). The cover letter should state the type of the article and tell which illustrations are original and which are not.

Notes: